



Fisheries and Oceans  
Canada

Pêches et Océans  
Canada

Ecosystems and  
Oceans Science

Sciences des écosystèmes  
et des océans

## **Canadian Science Advisory Secretariat (CSAS)**

---

**Research Document 2016/111**

**Quebec Region**

### **Describing krill distribution in the western North Atlantic using statistical habitat models**

Stéphane Plourde, Caroline Lehoux, Ian H. McQuinn, Véronique Lesage

Fisheries and Oceans Canada  
Institut Maurice-Lamontagne  
850, Route de la Mer  
Mont-Joli, Québec  
Canada G5H 3Z4

---

## Foreword

This series documents the scientific basis for the evaluation of aquatic resources and ecosystems in Canada. As such, it addresses the issues of the day in the time frames required and the documents it contains are not intended as definitive statements on the subjects addressed but rather as progress reports on ongoing investigations.

Research documents are produced in the official language in which they are provided to the Secretariat.

### Published by:

Fisheries and Oceans Canada  
Canadian Science Advisory Secretariat  
200 Kent Street  
Ottawa ON K1A 0E6

[http://www.dfo-mpo.gc.ca/csas-sccs/  
csas-sccs@dfo-mpo.gc.ca](http://www.dfo-mpo.gc.ca/csas-sccs/csas-sccs@dfo-mpo.gc.ca)



© Her Majesty the Queen in Right of Canada, 2016  
ISSN 1919-5044

### Correct citation for this publication:

Plourde, S., Lehoux, C., McQuinn, I.H., and Lesage, V. 2016. Describing krill distribution in the western North Atlantic using statistical habitat models. DFO Can. Sci. Advis. Sec. Res. Doc. 2016/111. v + 34 p.

---

---

## TABLE OF CONTENTS

ABSTRACT.....	IV
RÉSUMÉ .....	V
INTRODUCTION .....	1
MATERIALS AND METHODS .....	2
Krill historical data .....	2
Krill habitat models.....	2
Environmental variables .....	2
Generalized additive models .....	3
Prediction of significant areas of krill .....	4
RESULTS .....	4
Krill habitat models.....	4
Prediction of significant areas of krill .....	5
Overall occurrence of predicted dense krill aggregations .....	6
Category <i>Euphausiids</i> .....	6
Category <i>Meganyctiphanes norvegica</i> .....	6
Category <i>Thysanoessa</i> spp.....	6
<i>Euphausiids</i> on the eastern Newfoundland shelf .....	6
DISCUSSION.....	7
Krill habitat models.....	7
Prediction of significant areas of krill .....	8
Implications for the identification of the critical habitat of the blue whale .....	9
REFERENCES CITED.....	10
TABLES .....	14
FIGURES.....	16
APPENDIX.....	26

---

## ABSTRACT

The objective of this study was to describe the spatial distribution of krill in eastern Canadian waters using a statistical modelling approach in support of the identification of important habitat for the western North Atlantic (WNA) blue whale (*Balaenoptera musculus*). Generalized Additive Models (GAMs) were constructed from krill biomass data obtained during multifrequency acoustic surveys conducted in the Gulf of St. Lawrence (GSL) and a set of static (bathymetry and slope steepness) and satellite-derived dynamic (sea surface temperature, chlorophyll a biomass, sea level height anomalies) environmental correlates. GAMs were built for the spring and summer seasons for different krill taxa/categories. GAM results showed that environmental conditions promoting high krill biomass are species-specific and varied with season. Static and dynamic environmental variables were selected in all GAMs, indicating that dynamic oceanographic processes were important in controlling krill aggregations and distribution. GAMs predicted spatial patterns of krill biomass generally similar to those obtained with independent plankton net and acoustic data. GAMs were then used to predict 'Significant Aggregations of Krill' (SAK), i.e., areas where dense krill aggregations would have a greater probability of occurring. SAK cover less than 2% of the entire spatial domain and their location varied among krill categories and seasons. SAK were generally predicted in the lower St. Lawrence Estuary, along the Gaspé Peninsula and in the Shediac Valley, along the coast of southern and northeast Newfoundland, as well as along the slope of the deep channels in the GSL, off the Nova Scotian and Newfoundland continental shelves, and in the outer Bay of Fundy. These SAK are interpreted as areas where environmental conditions promote krill aggregation on a regular basis and therefore are potentially important for WNA blue whale foraging in eastern Canadian waters.

---

## Décrire la distribution de krill dans l'ouest de l'Atlantique Nord en utilisant des modèles statistiques d'habitats

### RÉSUMÉ

L'objectif de cette étude est de décrire la distribution spatiale du krill dans les eaux de l'est du Canada à l'aide de modèles statistiques, un travail réalisé en support à l'identification de l'habitat de la baleine bleue (*Balaenoptera musculus*) de l'ouest de l'Atlantique. Nous avons construit des modèles additifs généralisés (MAGs) à partir de données de biomasse de krill obtenues avec l'acoustique multifréquences lors de missions réalisées dans le golfe du Saint-Laurent (GSL) et un ensemble de données environnementales statiques (bathymétrie, pente du fond) et dynamiques estimées par imagerie satellitaire (température de surface, biomasse de chlorophylle *a*, anomalie de la hauteur de la surface). Les analyses à l'aide des MAGs ont été réalisées pour les saisons printanières et estivales ainsi que pour différentes catégories de krill. Les résultats montrent que la biomasse de chaque catégorie de krill répond de manière distincte aux conditions environnementales, une réponse variant également selon la saison. Des variables environnementales statiques et dynamiques contribuent dans les différents MAGs, démontrant l'importance des processus océanographiques dynamiques dans le contrôle de la distribution et l'occurrence des essaims de krill. Les MAGs permettent de prédire des patrons de distribution de la biomasse de krill correspondant de manière générale avec des données indépendantes. Par la suite, les MAGs ont été utilisés pour prédire les 'Régions d'Agrégation Significatives de Krill' (RASK), i.e. les régions où la probabilité de rencontrer des essaims denses de krill est la plus élevée. Les RASK ainsi déterminées ne représentent que 2 % de la superficie de la région d'étude et leur emplacement varie selon les catégories de krill et la saison. En général, les RASK sont prédites dans l'estuaire maritime du Saint-Laurent, le long de la péninsule gaspésienne et dans la vallée de Shediac, le long des côtes sud et est de Terre-Neuve, dans certaines régions situées sur la marge des chenaux profonds du GSL, sur le talus continental au large de la Nouvelle-Écosse et Terre-Neuve, ainsi qu'à l'entrée de la baie de Fundy. Ces RASK sont considérées comme des régions où les conditions environnementales permettent la formation d'essaims denses de krill sur une base régulière, représentant ainsi des régions potentiellement importantes pour l'alimentation de la baleine bleue de l'ouest de l'Atlantique.

---

## INTRODUCTION

Ecological, management and legal requirements reinforce the need to identify and protect important habitat for marine predators, especially those of species at risk, and has led to the propagation of spatially-explicit habitat models using a vast array of statistical approaches (Elith and Leathwick 2009, Aarts et al. 2012). Although food availability is obviously a key parameter for determining habitat quality for marine predators, in general only indirect proxies of prey density such as sea-surface physical (e.g. fronts, temperature) and biological (e.g. phytoplankton biomass) characteristics have been used in these models, with variable success (e.g., Forney et al. 2015, Willis-Norton et al. 2015). The relative weakness in predictive capacity of these indirect habitat variables is most likely because they are too many levels removed from the prey itself, given that the variability at each level is additive.

However, it is the lack of strong predictive capacity using prey field data which is the most concerning. This could arise for various reasons. Firstly, pelagic prey and predator data are rarely collected simultaneously, resulting in a temporal mismatch that minimizes the probability that any mechanistic predator-prey relationship will be captured with these data. Secondly, even when collected at the same time during surveys, the spatial resolution obtained using traditional point-sampling techniques (e.g., bongo and trawl net tows) to sample pelagic forage species such as mesozooplankton, krill and small fishes is in general considerably greater than the spatial and temporal scales that are meaningful for predators such as baleen whales. In addition, the scarcity of data for rarer species such as the endangered blue whale (*Balaenoptera musculus*) forces the use of observational data collected over multiple seasons, years and regions, with often no matching prey data.

For all of these reasons, researchers have advocated for the use of statistical models as the best approach to incorporate prey field distribution and abundance in predator habitat models (Torres et al. 2008, Aarts et al. 2014). In addition, the development of multifrequency acoustic techniques has enabled the continuous sampling of more detailed categories of prey groups over much larger areas compared to traditional station-sampling techniques. The description of areas of high prey density based on acoustically-derived prey biomass and predator observation data collected during synoptic surveys has contributed to the understanding of factors governing the distribution of marine birds (Santora et al. 2011), commercial fish stocks (Ressler et al. 2012), and baleen whales (Friedlaender et al. 2006, Santora et al. 2010, Ressler et al. 2015).

To identify the important habitat of WNA blue whales in eastern Canadian waters, our approach was therefore to describe statistically the spatial distribution of their principal prey, krill, while considering the stochastic nature of their distribution. Krill aggregations are often observed in the lower St. Lawrence Estuary (SLE) and Gulf of St. Lawrence (GSL), in the Scotian Shelf-Bay of Fundy (SS-BoF) region and off southern Newfoundland (NL) (McQuinn et al. 2015). However, the exact geographical position of these aggregations could vary substantially over time, reflecting the inherent variability of the complex bio-physical coupling between krill swimming behaviour and physical processes (Maps et al. 2014, Maps et al. 2015, Lavoie et al. 2015). In the GSL, the probability of observing discrete dense krill aggregations is greater in areas of surface convergence, suggesting that dynamic processes coupled to krill behaviour are significant for the formation and occurrence of these dense aggregations (Maps et al. 2015).

Our objectives were: (1) to build statistical habitat models using generalized additive models (GAM) from multifrequency acoustic data of krill collected during synoptic spatial surveys in the GSL along with environmental correlates, and (2) to use predictions from these habitat models to identify recurrent areas of high krill biomass over a multiyear period in the GSL, as well as in the SS-BoF and NL regions.

---

## MATERIALS AND METHODS

### KRILL HISTORICAL DATA

Krill biomass was estimated from multifrequency acoustic data (38, 70, 120, 200 kHz) collected during recent spatial surveys in the lower SLE and GSL (Fig. 1, 2). Two additional surveys with dual frequency acoustics (38, 120 kHz) were also performed, one in July in the SS-BoF and one in April off southern NL (Appendix 9). Multifrequency acoustic data were integrated in 0.5 km bins along the vessel track, affording a high-resolution quantification of biomass for different krill categories: (1) *Euphausiids* (= total krill), (2) *Meganyctiphanes norvegica* and (3) *Thysanoessa* spp. Only the more general category 'Plankton', shown to be dominated by krill and therefore considered as an equivalent of the *Euphausiids* category, was estimated from the dual frequency data (see McQuinn et al. 2015). *Thysanoessa* spp. included two common cold water species, *T. raschii* and *T. inermis*, and the rarer oceanic and warm water species, *T. longicaudata*. Technical details on the sampling and treatment of acoustic data are provided in McQuinn et al. (2013) and McQuinn et al. (2015).

### KRILL HABITAT MODELS

#### Environmental variables

We used a set of environmental variables shown or hypothesized to be important in the control of krill spatial and temporal distribution. These variables could be grouped into two categories:

- 1) Static: bathymetry (Bathy) and bottom slope steepness (Slope)

These variables are commonly included in habitat models of krill and other zooplankton because they can constrain their horizontal distribution through interaction with their vertical distribution and migrations. Bottom depth (Bathy) data was acquired from a 1 arc-minute global relief model (Amante and Eakins, 2009). Bottom slope (Slope) was calculated using the bathymetry of Amante and Eakins (2009). The slope steepness was calculated in degrees from 8 neighbouring cells using the algorithm of Horn (1981) implemented in R using the "raster" package (version 2.5-2, Hijmans, 2015).

- 2) Dynamic: Sea Surface Temperature (SST), chlorophyll *a* (CHLA), and mean sea level height anomalies (MSLA)

SST is a basic marine habitat parameter and is a proxy of the temperature regime influencing zooplankton productivity (biomass) and distribution at small and large spatial, and temporal scales. CHLA could be considered as a proxy of microplankton production and has often been used as a zooplankton habitat characteristic at large spatial scales in the open ocean (Santora et al. 2012, Albouy-Boyer et al. 2016). Finally, dense krill aggregations in the GSL have a greater probability of being associated with areas of high surface water convergence estimated by finite-time Lyapunov exponents (FTLE) computed from a 3-D physical model (Maps et al. 2015). However, a comparable modelling approach was not applicable for the spatial domain considered in our study because the operational 3-D physical model does not encompass the same region. However, MSLA has been used as a proxy of the circulation processes and dynamic features (fronts, gyres) that could accumulate planktonic organisms (Riquelme-Bugueño et al. 2015). MSLA derived from satellite imagery was therefore used as a substitute for FTLE.

Satellite imagery provided the dynamic environmental data at adequate temporal and spatial scales for our study. The monthly averages of the three dynamic variables were extracted from 2004 to 2014, inclusively. CHLA was extracted from MODIS Aqua Level 3 satellite images with

---

a resolution of 4 km (Ocean Biology Processing Group, 2003). MSLA daily anomalies were available in reference to a 20-year climatology (1993-2014) calculated from satellite images (available at <http://marine.copernicus.eu/>). The resolution of MSLA images was 0.2° Longitude/Latitude. Monthly SST were acquired as Level 3 satellite images ([resolution=0.015/0.01° Longitude/Latitude](#)). An example of the spatial patterns for all static and dynamic environmental variables is shown in Appendix 1.

The spatial resolution of satellite imagery data is not ideal for the upstream half of the lower SLE, a region where krill aggregations are regularly observed. This limitation was judged minor considering (1) the need to describe krill spatial distribution over a wide region, including areas where very little is known on krill distribution, and (2) blue whales are known to use the upper half of the lower SLE, a region where krill aggregation dynamics has been intensively studied in the past (Simard et al. 1986, Simard and Lavoie 1999, Lavoie et al. 2000).

### Generalized additive models

Two seasons (spring, summer) were considered in building the GAMs to account for seasonal changes in krill behaviour and growth, and in the main circulation regime resulting from changes in the dominant wind direction in mid-summer (Maps et al. 2011, Lavoie et al. 2015).

Krill biomass and environmental variables were converted to a 10 x 10 km grid. Then, the maximum biomass value observed in each grid cell from all the surveys was extracted. Environmental data were resampled according to the same grid using the mean value in each cell. Krill biomass data collected in areas deeper than 600 m or shallower than 10 m were excluded from the analyses because of their extremely low occurrence in the data set.

GAMs were fitted using R and the “mgcv” (v. 1.8.10, Woods, 2015) package (version 3.1.0, 2014), assuming a Gaussian distribution. The response variable (krill biomass) was normalized using  $x^{1/5}$ . The number of degrees of freedom was limited to  $\leq 3$  for the SST,  $\leq 5$  for Bathy and  $\leq 4$  for CHLA, Slope and MSLA to avoid multimodal relationships and to obtain biologically interpretable effects (Albouy-Boyer et al. 2016). Although we did run GAMs with unlimited degrees of freedom, these runs did not result in better model fits while showing effects from predictors sometimes difficult to reconcile with krill biology (not shown). A GAM was fitted for each krill category (dual frequency: *Plankton*; multifrequency: *Euphausiids*, *M. norvegica*, *Thysanoessa* spp.) for each of the two seasons (spring, summer). Data in May and June were used to fit spring models and those acquired in August and September were used to fit summer models. Dual frequency acoustic surveys conducted in April off southern NL, and in July in the SS-BoF were used in the spring and summer *Plankton* models, respectively. Krill data were fitted using the monthly mean of environmental variables corresponding to the month and year when each acoustic survey was conducted.

Optimal GAMs were selected by computing models with every possible combination of the five environmental variables using the “MuMin” package (version 1.15.6, Barton, 2016). For each of the ten iterations ran for each model, a random sample of 70% of the data set was used to fit the model and the remaining 30% to evaluate model performance. Variables were selected to minimize the AIC and maximize the Spearman rank correlation coefficient. The optimal model included variables that were, on average, more frequently selected after 10 iterations. The final model was refitted on 100% of the data. For more details on this procedure see Albouy-Boyer et al. (2016).

Model residuals were inspected for normality, homogeneity and spatial autocorrelation (SA). SA was verified with the Moran’s I using the R package “spdep” (version 0.5-92, Bivand, 2015). Contiguity was evaluated by nearest neighbors within a distance of 11 km to ensure complete connectivity. SA was generally significant at lag 1 ( $I < 0.4$ ), and lag 2 ( $I < 0.3$ ). The SA value is



---

the result of the aggregation of krill and decreased when the resolution of the grid was adjusted to 20 km. Moreover, the presence SA did not result in a biasing of predictions, as suggested by the strong similarity between predictions from models fitted with 10 and 20 km grids (not shown).

## PREDICTION OF SIGNIFICANT AREAS OF KRILL

Optimal GAMs were used to predict krill biomass distribution in the SS-BoF, GSL and NL regions. Because of the inherent variability in the distribution of krill aggregations, we chose an approach considering the probability for a dense krill aggregation to be observed in any given location, i.e. a dynamic 'preyscape'.

Environmental variables were resampled on a 10-km grid with an extent of -72.5 to -35° in longitude and 42 to 58 ° in latitude. One grid (10 x 10 km) was generated for each of the months of May, June, July, August and September for each year from 2009 to 2013. The months of May and June were used to predict the response using the spring models whereas the months of July, August and September were used with the summer models. Our predictions were therefore based on 10 (2 months\*5 years) and 15 (3 months\*5 year) replicates for the spring and summer periods, respectively.

Our approach included three steps:

- (1) For each replicate (month\*year), cells with a predicted biomass >95<sup>th</sup> percentile across the model domain were selected. This 'relative' threshold was used because GAMs predict the average response of the dependent variable to variations in environmental conditions, not its extremes as are the denser krill aggregations. It also corresponds to the proportion of krill biomass data that were above a density threshold of 100 g m<sup>-2</sup> in 2005 and 2007 in the GSL (Goldbogen et al. 2011, Maps et al. 2015);
- (2) For each cell, the number of replicates (month\*year) with a predicted biomass > 95<sup>th</sup> percentile was calculated;
- (3) Results were mapped according to three categories based on the occurrence of biomass > 95<sup>th</sup> percentile, i.e. cells with no occurrence, cells with less than 50% of occurrence, and cells with more than 50% of occurrence. Cells with a probability greater than 50% for a dense krill aggregation to occur were defined as 'Significant Areas of Krill' (SAK).

## RESULTS

### KRILL HABITAT MODELS

Optimal GAM results are summarized in Table 1 and 2, and response curves of models used for predicting dense krill aggregations (see below) are presented in Appendix 2-7. Every static (Bathy, Slope) and dynamic (SST, CHLA, MSLA) environmental variables contributed (but not necessarily in all models) to explain the deviance in krill biomass distribution (Table 1).

Slope was a significant variable in all GAMs (Table 1). Additionally, the effect of Bathy and Slope on biomass differed among *M. norvegica* and *Thysanoessa* spp. and seasons (Table 2). *M. norvegica* biomass was positively affected by bathymetry between 69-324 m in spring and 74-473 m in fall, whereas depths between 56-172 m and 60-200 m showed a positive effect on *Thysanoessa* spp. biomass in spring and summer, respectively (Table 2). A change in the range of slope values showing a positive effect on biomass accompanied these changes in bathymetry (Table 2).

---

While SST was not selected as a significant variable for *M. norvegica* in spring (Table 1), biomass of this species was positively influenced by SST between 9.8 and 16°C in summer (Table 1). For *Thysanoessa* spp., abundance was greater at SST above 10.5°C in spring and between 11.2°C and 16.2°C in summer (Table 2). Therefore, biomass of both krill species was negatively affected at SST greater than 16°C.

The different krill categories responded similarly to MSLA when selected (Table 1, Table 2). A positive effect on krill biomass was shown over a smaller range of MSLA values in spring relative to summer, but maximum MSLA values were similar in both seasons (Table 2). This pattern suggests that dense krill aggregations in spring were more associated with specific and high MSLA values (i.e., frontal regions) than during summer.

High krill biomass was associated with high surface CHLA biomass when this variable was included in the GAMs (Table 1, Table 2). The lower threshold CHLA value was greater in summer than in spring, whereas the maximum value was lower for *M. norvegica* than for *Thysanoessa* spp. (Table 2).

GAM results were similar among the three krill biomass categories estimated from multifrequency acoustic data (*Euphausiids*, *M. norvegica* and *Thysanoessa* spp.) with the range of environmental variables promoting high biomass either corresponding to the range described for a particular species or to an average of both species (Table 1, Table 2). GAMs built with the more general *Plankton* category estimated from dual frequency acoustic data did perform well, but not as well as those with krill categories estimated with multifrequency data (Table 1). Although the effect of environmental variables was generally similar to those obtained with other models, their poorer predictive power was perhaps caused by a poorer discrimination of the krill signal from other important components of the pelagic community. For this reason, we decided not to use this category further in our study.

## PREDICTION OF SIGNIFICANT AREAS OF KRILL

In general, the confidence intervals around the modelled effect of each environmental variable on krill biomass increased at both ends of their data range where observations were less abundant (see Appendix 2-7). We were therefore careful not to stretch our predictions beyond the range of environmental data included in the GAMs to minimize the uncertainty around the predictions as is inherent to every statistical approach (Brun et al. 2016). Consequently, areas shallower and deeper than 10 m and 600 m, respectively, and with slope greater than 1.5° were not considered in our predictions (see Appendix 2-7). This conservative approach had the advantage of minimizing the uncertainty of the krill biomass predictions but with the drawback of excluding the margin of the continental shelf from the spatial domain considered in our predictions.

Biomass of the *Euphausiids* category predicted for June 2012 is presented as an example of predictions made with the GAMs (Fig. 3). In this GAM, the environmental seascape included two static variables, Bathy and Slope, and two dynamic variables, MSLA and CHLA (Table 2). The GAM predicted strong spatial gradients resulting in a spatial pattern previously observed with historical acoustic data not included in our analyses in the lower SLE and western GSL (McQuinn et al. 2015). It also predicted greater krill biomass in deep basins on the eastern SS (relative to surrounding waters) although predicted biomasses were markedly lower than in the GSL (Fig. 3).

Predictions were made for the spring and summer periods with GAMs built for *Euphausiids*, *M. norvegica* and *Thysanoessa* spp. Significant Areas of Krill (SAK) were specifically identified. Results are first represented for the spatial domain covered by krill historical data, i.e., the GSL,

---

SS-BoF and off southern NL. Predictions for the *Euphausiids* category on the eastern NL shelf outside the spatial domain for which we had krill biomass data are presented separately.

### **Overall occurrence of predicted dense krill aggregations**

Considering all models, cells with at least one predicted dense krill aggregation represented only 10% of the spatial domain. Among these cells, 25% were SAK (>50% of occurrence), whereas only 4% showed a 100% probability for a dense krill aggregation to occur. Over the entire spatial domain, SAK represented only 2% of the total number of cells. A more detailed description of the predictions from the different models is provided below.

### **Category *Euphausiids***

In spring, SAK represented 32% of all cells where at least one dense *Euphausiids* aggregation was predicted (Appendix 8). In the GSL, large SAK occupying several contiguous 10 X 10 km cells were organized as a continuum along the southern coast of the lower SLE and along the Gaspé Peninsula into the Shediac Valley, along the coast of the northern GSL and around Anticosti Island (Fig. 4). Large SAK were also predicted at the head of Esquiman channel in the eastern GSL, in the outer BoF and in the western Gulf of Maine. Smaller SAK were also predicted on the eastern SS and off southern NL.

In summer, SAK represented 27% of locations where at least one dense aggregation of *Euphausiids* was predicted (Appendix 8). Several large SAK that were observed in spring in the lower SLE, in the GSL and in the Gulf of Maine/ BoF appeared smaller in the summer with a more fragmented distribution (Fig. 5). Contrary to the GSL, large SAK occupying several contiguous cells were predicted off southern NL, while smaller ones appeared on the eastern SS and in the Gully (Fig. 5).

### **Category *Meganyctiphanes norvegica***

Prediction of SAK for *M. norvegica* varied greatly among seasons (Fig. 6, 7). SAK represented 38% and 8% of cells with at least one dense aggregation in spring and summer respectively (Appendix 8). In spring, SAK spatial distribution resembled the one for the *Euphausiids* category (eg: in the lower SLE and western GSL, on the eastern SS), but also showed differences with several small SAK predicted along the slopes of deep channels (Fig. 6). In summer, SAK were mostly restricted to the lower SLE, western GSL and off southern NL (Fig. 7).

### **Category *Thysanoessa* spp.**

Prediction of SAK for *Thysanoessa* spp. also varied among seasons (Fig. 8, 9). The proportion of cells where at least one dense aggregation was predicted and estimated to be a SAK was greater in summer (31%) than in spring (17%) (Appendix 8). In spring, SAK were located in coastal areas near Anticosti Island and in the northeast GSL (Fig. 8). In summer, SAK were generally larger and formed a continuum in several areas similarly to those described for the *Euphausiids* category (Fig. 9). Large SAK also were predicted in the lower SLE and in different sub-regions of the GSL, off southern NL, on the SS and in the outer BoF (Fig. 9).

### ***Euphausiids* on the eastern Newfoundland shelf**

In spring, GAM predicted very few areas of biomass >95<sup>th</sup> percentile (Fig. 10) in eastern NL where we had no corresponding krill biomass data. However, several SAK were predicted in eastern NL waters with the summer GAM built for the *Euphausiids* category (Fig. 10). SAK were predicted at the shelf break around the Grand Banks and offshore around Flemish Cap, but also on the inner and outer shelf in northern areas (Fig. 10).

---

## DISCUSSION

### KRILL HABITAT MODELS

Overall, our results showed that the performance of our habitat model was comparable to other studies on krill biomass distribution using GAMs (i.e., Santora et al. 2012, Riquelme-Bugueño et al. 2015, Silk et al. 2016). Static and dynamic environmental variables were selected in all GAMs. In our framework, static environmental variables could be seen as obligatory for a krill aggregation to occur through their influence in modulating background circulation patterns. Dynamic environmental variables represent proxies for processes influencing the pattern of krill patches by determining the spatial distribution and density of krill aggregations at finer spatiotemporal scales. Our results also highlighted the importance of considering species-specific responses to environmental conditions as well as seasonal variations in environmental forcing.

The effect of static environmental variables on krill biomass varied among species and seasons. The effect of bathymetry and slope steepness on krill biomass was species-specific, likely reflecting the different daytime optimal depth observed in the GSL, deeper for *M. norvegica* and shallower for *Thysanoessa* spp. (Plourde et al. 2014, McQuinn et al. 2015). Additionally, the effect of bathymetry varied among seasons, with high biomass of all krill categories being associated to deeper regions in the summer compared to spring. This seasonal difference could be associated with a deepening of krill daytime depth in response to a greater light penetration in summer than in spring following a seasonal decrease in the input of freshwater loaded with dissolved organic matter from the St. Lawrence River and other tributaries (Plourde et al. 2014).

The positive effect of MSLA did confirm the importance of considering dynamic circulation in krill habitat models (Santora et al. 2012, Riquelme-Bugueño et al. 2015). Moreover, indices of ocean surface structures (eg: fronts, gyres, etc...) have been used as proxies of potential planktonic and small pelagic prey availability in several habitat models of top marine predators (i.e., Torres et al. 2008). Using an index such as MSLA derived from satellite imagery, our results confirmed previous results obtained with finite-time Lyapunov exponents (FTLE) calculated from a 3-D physical model showing the importance of convergence areas to promote krill aggregations in the GSL (Maps et al. 2015). Similarly to the static environmental variables, the effect of MSLA on krill biomass varied between seasons. The observed change in the range of values for MSLA between spring and summer that positively affect krill biomass could reflect a change in the coupling between krill behaviour and circulation. This change in coupling could be associated with the biologically-driven modification of krill swimming behaviour and vertical distribution caused by changes in reproduction state and feeding mode e.g. herbivory vs carnivory, following the end of the bloom period (Sameoto 1980, Nicol 1984, Lass et al. 2001).

While MSLA would reflect the effect of physical dynamic processes on krill aggregations, SST and CHLA should be interpreted as environmental factors affecting the overall krill population dynamics and productivity. SST in the GSL in spring had little effect on krill biomass due to generally cooler conditions (See Table 2). However under the wider SST range observed in the warmer summer, our GAMs revealed that SST greater than 16°C would have a negative effect on the biomass of all three categories of krill in the GSL. A 16°C SST in summer corresponds to 12-14°C averaged over the 0-50 m layer in eastern Canadian waters, the depth layer generally occupied by migrating sub-Arctic copepods and krill that are actively foraging during nighttime in the region (Simard et al. 1986, Souriseau et al. 2008, Maps et al. 2011). Interestingly, temperatures above 12°C could negatively affect the metabolisms of cold water krill species such as *T. raschii* and *T. inermis*, whereas the same conditions may not affect the metabolism of *M. norvegica* (Huenerlage and Bucholz 2015). SST could also be indicative of more global ecological processes regulating zooplankton mortality and survival in general, e.g. daily

---

mortality rate of the dominant sub-Arctic *Calanus finmarchicus* is also positively related to temperature (Plourde et al. 2009, Melle et al. 2014). Such relationships are unknown for krill, but the negative effect of SST >16°C (or 12-14°C in the 0-50 m layer) on krill biomass in summer could reflect similar ecological processes. The significant effect of CHLA on krill biomass should reflect a general association between physical processes favouring krill aggregation and areas of greater primary production (e.g. upwelling zones along the coast in the northern GSL; Appendix 1) but also a direct effect on krill growth and recruitment at the monthly scale considered in the GAMs.

## **PREDICTION OF SIGNIFICANT AREAS OF KRILL**

Our GAMs predicted high biomass values (> 95<sup>th</sup> percentile of predicted values) for at least one month in the 2009-2014 period in 10% of the spatial domain. However, SAK (areas predicted with a probability >50% for a biomass >95<sup>th</sup> percentiles) occurred over a much smaller area, representing 25% of the high biomass area, and 2% of the entire spatial domain. Variations in the probability of high density values predicted in each grid cell were caused by variations in dynamic environmental variables (SST, CHLA, MSLA), probably reflecting the interaction between the dynamic environmental forcing and krill diel vertical migrations. Therefore, the concept of SAK developed in this study would be more relevant to the description of the dynamic krill preyscape than predictions of krill biomass itself.

Our models did predict dense augmented krill aggregations and SAK in deep basins on the eastern SS, but not in basins on the western SS. Basins on the SS have been the focus of a few krill studies between the mid 1980's and mid 1990's (Cochrane et al. 1991, Sameoto et al. 1993). However as for other areas, their relevance for describing krill population dynamics at the scale of eastern Canadian had never been evaluated. The spatial distribution of dense krill aggregations summarized in Appendix 9 using data not included in our GAMs suggests that krill biomass was not substantial in the basins of the western SS in 2012. SST is generally increasing on the SS, and inflow of warmer deep slope waters onto the western SS has occurred more frequently over the past few years, affecting bottom temperature in the region (Hebert et al. 2013). These changes in oceanographic conditions were accompanied by an increase in abundance of warm-water, offshore copepod species, and a decrease in sub-Arctic and Arctic copepod species (Johnson et al. 2016). Consequently, the western SS might have become less suitable for the cold-water krill species targeted in our study.

There is an inherent uncertainty around the predictions made with habitat models and it is generally recommended to limit predictions to the geographic range and time period included in the data used to build these models (Heikkinen et al. 2012). In our study, we did limit predictions of krill biomass from GAMs built with data collected in the GSL to the range of static environmental correlates well represented in our data, i.e. depths between 10 and 600 m and slope < 1.5°, a range over which the effect of these variables on krill biomass included small confidence intervals (Appendix 2-7). GAMs have been shown to be the regression-based method with the best transferability capacity and that habitat models based on abundance appear to outperformed those based on presence/absence data (Araujo et al. 2005, Heikkinen et al. 2012, Howard et al. 2014). Therefore, our decision to use GAMs built with biomass data and to limit the predictions to the environmental data range for which the models best performed suggests that predictions made outside the GSL should be reliable. Furthermore, comparison with independent krill data suggests that our predictions are generally consistent with our current knowledge of krill distribution in the region. In the GSL, predicted SAKs correspond in large part to the high convergence zones where krill aggregations were observed with a greater probability in August 2005 and 2007 than in the rest of the GSL (Maps et al. 2015). Moreover,

---

the location of dense krill aggregations previously observed in the GSL during synoptic spatial surveys also corresponds to areas where SAK were predicted (McQuinn et al. 2015).

In the SS-BoF region and off southern NL, SAKs roughly correspond to areas of dense krill biomass based on data collected with a dual acoustic system during two surveys that were not included in our GAMs (see Appendix 9). On the eastern and northern NL shelf, the lack of krill biomass data precluded any validation of our predictions made in this region and should therefore be interpreted with caution. As previously mentioned, the statistical limitation of our approach prevented predictions of krill biomass and SAK in the deeper continental slope region (depth >600 m, slope > 1.5°), a region where blue whales have historically been observed and which could contain important foraging habitat for this species (Appendix 9).

The transferability of our GSL-based krill habitat models to other regions could also be influenced by changes in krill biology and species composition that could affect relationships with environmental correlates described in our GAMs. Although consistent krill taxonomic and biomass data are generally lacking on the SS and in the NL region, one would expect that the large gradient in environmental conditions across the eastern Canadian Atlantic region would affect krill species composition on the SS, NL and in deeper continental slopes regions relative to the GSL. GAMs built with the more general *Plankton* category estimated from dual frequency acoustic did not perform as well as those with distinct krill taxa estimated with multifrequency data (see Table 1). As a consequence, it appears essential to analyse existing or newly acquired multifrequency acoustic data validated with biological samples from the SS and NL to improve krill habitat models and potentially the prediction of SAK in the SS and NL regions, particularly on the continental slope area.

In conclusion, one must remember that krill transport and aggregation are highly dynamic processes and are the reflection of a pelagic habitat varying at different spatial and temporal scales. Statistical habitat modelling has been widely used to describe species distribution and responses to potential changes in environmental conditions in the ocean, but are inherently limited by the spatial and temporal scales of available data that rarely correspond to the scales at which processes determining species abundance and distribution are operating (i.e., Torres et al. 2008). Because of this, our statistical modelling approach and SAK determination which considered variations in dynamic environmental variables on a monthly scale is a step forward, but might not be optimal for matching krill biomass field data collected during synoptic surveys. Attempting other temporal integration scales for environmental data might improve our results. Despite their own limitations, 3-D coupled bio-physical models of krill life history including the swimming behaviour modulated by key biological processes (reproduction, moulting, feeding) could be a complementary tool to address questions related to biological-physical coupling processes such as those involved in the control of krill biomass and SAK formation in the region.

## **IMPLICATIONS FOR THE IDENTIFICATION OF THE CRITICAL HABITAT OF THE BLUE WHALE**

Because of its ecological significance, food availability has been advocated as a key habitat characteristic for large marine predators but has rarely been considered in habitat modelling due to a lack of adequate data. When available in the past, pelagic prey data have not substantially improved large marine predator habitat models, most likely because synoptic prey distribution data does not adequately represent the inherent spatio-temporal scales and variability characteristic of the pelagic foraging habitat of large predators (i.e., Torres et al. 2008). Consequently, most studies of large marine predator habitat and distribution have used indirect oceanographic proxies thought to represent processes that would drive prey distribution and density. However, it has been proposed that predictive modelling of prey distribution could

---

represent a better tool to estimate prey availability in large marine predator habitat models (Torres et al. 2008, Aarts et al. 2014).

This study was performed in the context of determining important foraging habitat for the WNA blue whale population in eastern Canadian waters. Our assumption was that the krill preyscape would be a key feature of blue whale foraging habitat and spatial distribution from spring to fall in eastern Canadian waters. We elected to use a statistical modelling approach capturing the fundamental characteristics of krill habitat, including the dynamic surface circulation processes likely involved in the formation, transport and disruption of krill aggregations (Maps et al. 2015). Our statistical modelling approach allowed for the optimal use of synoptic spatial krill biomass data collected at high spatial resolution with multi-frequency acoustic methods and available environmental data. The dynamic dimension included in our statistical models allowed the prediction of a dynamic krill preyscape based on the probability for a whale to encounter a high biomass krill patch at any location in spring and summer within the region. Despite the inherent uncertainty associated with predictions made using statistical habitat models, this study represents a significant step forward in developing a comprehensive approach for the understanding of ecological drivers of large marine mammal distribution, population dynamics, and habitat use.

## REFERENCES CITED

- Aarts, G.M., Jones, E., Brasseur, S.M.J.M., Rindorf, A., Smout, S.C., Dickey-Collas, M., Wright, P., Russell, D., McConnell, B.J., Kirkwood, R.J., Fedak, M., Matthiopoulos, J., Reijnders, P.J.H. 2014. Prey habitat model outperforms prey data in explaining grey seal distribution. In : 28th Annual Conference European Cetacean Society, Liege, Belgium, September 2014.
- Aarts, G., Fieberg, J., Matthiopoulos, J. 2012. Comparative interpretation of count, presence–absence and point methods for species distribution models. *Meth. Ecol. Evol.*, 3: 177-187.
- Albouy-Boyer, S., Plourde, S., Pepin, P., Johnson, C., Lehoux, C., Galbraith, P. S., Hebert, D., Lazin, G., Lafleur, C. 2016. Habitat modelling of key copepod species in the Northwest Atlantic Ocean based on the Atlantic Zone Monitoring Program. *J. Plank. Res.*, 38: 589–603, doi:10.1093/plankt/fbw020.
- Amante, C. and Eakins, B.W. 2009. ETOPO1 1 Arc-Minute Global Relief Model: Procedures, Data Sources and Analysis. NOAA Technical Memorandum NESDIS NGDC-24. National Geophysical Data Center, NOAA. doi:10.7289/V5C8276M.
- Araújo, M. B., Pearson, R. G., Thuiller, W., Erhard, M. 2005. Validation of species–climate impact models under climate change. *Global Change Biol.*, 1: 1504-1513.
- Barton, K. 2016. MuMIn: Multi-Model Inference. R package version 1.15.6.
- Bivand, R. 2015. Spatial Dependence: Weighting Schemes, Statistics and Models. R package version 0.5-92.
- Brun, P., Kjørboe, T., Licandro, P., Payne, M. R. 2016. The predictive skill of species distribution models for plankton in a changing climate. *Global Change Biol.* Doi: 10.1111/gcb.13274.
- Cochrane, N. A., Sameoto, D., Herman, A. W., Neilson, J. 1991. Multiple-frequency acoustic backscattering and zooplankton aggregations in the inner Scotian Shelf basins. *Canadian J. Fish. Aquat. Sci.*, 48: 340-355.
- Elith, J., and Leathwick, J.R. 2009. Species distribution models: ecological explanation and prediction across space and time. *Annu. Rev. Ecol. Evol. Syst.* 2009. 40: 677–97.

- 
- Forney, K. A., Becker, E. A., Foley, D. G., Barlow, J., Oleson, E. M. 2015. Habitat-based models of cetacean density and distribution in the central North Pacific. *Endang. Species Res*, 27: 1-20.
- Friedlaender, A. S., Halpin, P. N., Qian, S. S., Lawson, G. L., Wiebe, P. H., Thiele, D., Read, A. J. 2006. Whale distribution in relation to prey abundance and oceanographic processes in shelf waters of the Western Antarctic Peninsula. *Mar. Ecol. Prog. Ser.*, 317: 297–310.
- Goldbogen, J. A., Calambokidis, J., Oleson, E., Potvin, J., Pyenson, N. D., Schorr, G., Shadwick, R. E. 2011. Mechanics, hydrodynamics and energetics of blue whale lunge feeding: efficiency dependence on krill density. *J.J. Exp. Biol.*, 214: 131-146.
- Hebert, D., R. Pettipas, D. Brickman, Dever, M. 2013. [Meteorological, Sea Ice and Physical Oceanographic Conditions on the Scotian Shelf and in the Gulf of Maine during 2012](#). DFO Can. Sci. Advis. Sec. Res. Doc. 2013/058. v + 46 p.
- Heikkinen, R. K., Marmion, M., Luoto, M. 2012. Does the interpolation accuracy of species distribution models come at the expense of transferability?. *Ecography*, 35: 276-288.
- Hijmans Robert J. 2015. Raster: Geographic Data Analysis and Modeling. R package version 2.5-2.
- Horn, B.K.P., 1981. Hill shading and the reflectance map. *Proceedings of the IEEE*, 69:14-47.
- Howard, C., Stephens, P. A., Pearce-Higgins, J. W., Gregory, R. D., Willis, S. G. 2014. Improving species distribution models: the value of data on abundance. *Meth.Ecol. and Evol.*, 5: 506-513.
- Huenerlage, K., and Buchholz, F. 2015. Thermal limits of krill species from the high Arctic Kongsfjord (Spitsbergen). *Mar. Ecol. Prog. Ser.*, 535: 89-98.
- Johnson, C., Casault, B., Head, E., Spry, J. 2016. [Optical, Chemical, and Biological Oceanographic Conditions on the Scotian Shelf and in the Eastern Gulf of Maine in 2014](#). DFO Can. Sci. Advis. Sec. Res. Doc. 2016/003. v + 51 p.
- Lass, S., Tarling, G. A., Virtue, P., Matthews, J. B., Mayzaud, P., Buchholz, F. 2001. On the food of northern krill *Meganyctiphanes norvegica* in relation to its vertical distribution. *Mar. Ecol. Prog. Ser.*, 214: 177-200.
- Lavoie, D., Simard, Y., Saucier, F. J. 2000. Aggregation and dispersion of krill at channel heads and shelf edges: the dynamics in the Saguenay-St. Lawrence Marine Park. *Can. J. Fish. Aquat. Sci.*, 57: 1853-1869.
- Lavoie, D., Chassé, J., Simard, Y., Lambert, N., Galbraith, P.S., Roy, N., Brickman, D. 2015 Large-Scale Atmospheric and Oceanic Control on Krill Transport into the St. Lawrence Estuary Evidenced with Three-Dimensional Numerical Modelling. *Atmosphere-Oceans*, 53: 1-27.
- Maps, F., Zakardjian, B. A., Plourde, S., Saucier, F. J. 2011. Modeling the interactions between the seasonal and diel migration behaviors of *Calanus finmarchicus* and the circulation in the Gulf of St. Lawrence (Canada). *J. Mar. Syst.*, 88: 183-202.
- Maps, F., Plourde, S., Lavoie, D., McQuinn, I., Chassé, J. 2014. Modelling the influence of daytime distribution on the transport of two sympatric krill species (*Thysanoessa raschii* and *Meganyctiphanes norvegica*) in the Gulf of St Lawrence, eastern Canada. *ICES J. Mar. Sci.*, 71: 282-292, doi:10.1093/icesjms/fst021.
-



- 
- Maps, F., Plourde, S., McQuinn, I. H., St-Onge-Drouin, S., Lavoie, D., Chassé, J., Lesage, V. 2015. Linking acoustics and finite-time Lyapunov exponents reveals areas and mechanisms of krill aggregation within the Gulf of St. Lawrence, eastern Canada. *Limnol. Oceanogr.*, 60: 1965-1975.
- McQuinn, I. H., Dion, M., St-Pierre, J. F. S. 2013. The acoustic multifrequency classification of two sympatric euphausiid species (*Meganyctiphanes norvegica* and *Thysanoessa raschii*), with empirical and SDWBA model validation. *ICES J. Mar. Sci.*, 70: 636-649.
- McQuinn, I. H., Plourde, S., St-Pierre, J. F. S., Dion, M. 2015. Spatial and temporal variations in the abundance, distribution, and aggregation of krill (*Thysanoessa raschii* and *Meganyctiphanes norvegica*) in the lower estuary and Gulf of St. Lawrence. *Prog. Oceanogr.*, 131: 159-176.
- Melle, W., Runge, J.A., Head, E., Plourde, S., Castellani, C., Licandro, P., Pierson, J., Jonasdottir, S.H., Johnson, C., Broms, C., Debes, H., Falkenhaus, T., Gaard, E., Gislason, A., Heath, M.R., Niehoff, B., Nielsen, T.G., Pepin, P., Stenevik, E.K., Chust, G. (2014) The North Atlantic Ocean as habitat for *Calanus finmarchicus*: environmental factors and life history traits *Prog. Oceanogr.*, 129 : 244–284.
- Nicol, S. 1984. Population structure of daytime surface swarms of the euphausiid *Meganyctiphanes norvegica* in the Bay of Fundy. *Mar. Ecol. Prog. Ser.*, 18: 241-251.
- Ocean Biology Processing Group. 2003. [MODIS Aqua Level 3 Global Monthly Mapped 4 km Chlorophyll a](#). Ver. 6. PO.DAAC, CA, USA. Dataset accessed [2016-01-20].
- Plourde, S., Pepin, P., Head, E. 2009. Long-term seasonal and spatial patterns in mortality and survival of *Calanus finmarchicus* across the Atlantic Zone Monitoring Program region, Northwest Atlantic. *ICES J. Mar. Sci.*, 66: 1942–1958.
- Plourde, S., McQuinn, I. H., Maps, F., St-Pierre, J. F., Lavoie, D., Joly, P. 2014. Daytime depth and thermal habitat of two sympatric krill species in response to surface salinity variability in the Gulf of St Lawrence, eastern Canada. *ICES J. Mar. Sci.*, 71: 272-281.
- Ressler, P.H., De Robertis, A., Warren, J.D., Smith, J.N., Kotwicki, S. 2012. Developing and acoustic survey of euphausiids to understand trophic interactions in the Bering Sea ecosystem. *Deep-Sea Res. (II)*, 65–70: 184–195.
- Ressler, P. H., Dalpadado, P., Macaulay, G. J., Handegard, N., Skern-Mauritzen, M. 2015. Acoustic surveys of euphausiids and models of baleen whale distribution in the Barents Sea. *Mar. Ecol. Prog. Ser.*, 527: 13-29.
- Riquelme-Bugueño, R., Correa-Ramírez, M., Escribano, R., Núñez, S., Hormazábal, S. 2015. Mesoscale variability in the habitat of the Humboldt Current krill, spring 2007. *J. Geophysical Res.: Oceans*, 120: 2769-2783.
- Sameoto, D. D. 1980. Relationships between stomach contents and vertical migration in *Meganyctiphanes norvegica*, *Thysanoessa raschii* and *T. inermis* (Crustacea Euphausiacea). *J. Plank. Res.*, 2: 129-143.
- Sameoto, D., Cochrane, N., Herman, A. 1993. Convergence of acoustic, optical, and net-catch estimates of euphausiid abundance: use of artificial light to reduce net. *Can. J. Fish. Aquat. Sci.*, 50: 334-346.
- Santora, J. A., Reiss, C. S., Loeb, V. J., Veit, R. R. 2010. Spatial association between hotspots of baleen whales and demographic patterns of Antarctic krill *Euphausia superba* suggests size-dependent predation. *Mar. Ecol. Prog. Ser.*, 405: 255-269.
-

- 
- Santora, J. A., Ralston, S., Sydeman, W. J. 2011. Spatial organization of krill and seabirds in the central California Current. *ICES J. Mar. Sci.*, 68: 1391–1402.
- Santora, J. A., Sydeman, W. J., Schroeder, I. D., Reiss, C. S., Wells, B. K., Field, J. C., Loeb, V. J. 2012. Krill space: a comparative assessment of mesoscale structuring in polar and temperate marine ecosystems. *ICES J. Mar. Sci.*, 69: 1317-1327.
- Silk, J. R., Thorpe, S. E., Fielding, S., Murphy, E. J., Trathan, P. N., Watkins, J. L., Hill, S. L. 2016. Environmental correlates of Antarctic krill distribution in the Scotia Sea and southern Drake Passage. *ICES J. Mar. Sci.*, fsw097.
- Simard, Y., Lacroix, G., Legendre, L., 1986. Diel vertical migrations and nocturnal feeding of a dense coastal krill scattering layer (*Thysanoessa raschi* and *Meganctyphanes norvegica*) in stratified surface waters. *Mar. Biol.*, 91: 93–105.
- Simard, Y., Lavoie, D., 1999. The rich krill aggregation of the Saguenay – St. Lawrence Marine Park: hydroacoustic and geostatistical biomass estimates, structure, variability and significance for whales. *Can. J. Fish. Aquat. Sci.*, 56:1182–1197.
- Sourisseau, M., Simard, Y., Saucier, F. J. 2008. Krill diel vertical migration fine dynamics, nocturnal overturns, and their roles for aggregation in stratified flows. *Can. J. Fish. Aquat. Sci.*, 65: 574-587.
- Torres, L. G., Read, A. J., Halpin, P. 2008. Fine-scale habitat modeling of a top marine predator: do prey data improve predictive capacity. *Ecol. Applications*, 18: 1702-1717.
- Willis-Norton, E., Hazen, E. L., Fossette, S., Shillinger, G., Rykaczewski, R. R., Foley, D. G., Bograd, S. J. 2015. Climate change impacts on leatherback turtle pelagic habitat in the Southeast Pacific. *Deep Sea Res. (II)*, 113: 260-267.
- Woods. 2015. *Mgcv*:Mixed GAM Computation Vehicle with GCV/AIC/REML Smoothness Estimation. R package version 1.8.10.

## TABLES

Table 1: Optimal GAMs based on different categories of krill biomass data. See text for the description of abbreviations used for environmental variables.

Season	Category	Formula	N	intercept	GCV	%DEV	r
<b>Spring</b>	Plankton	Biomass ~ log(ChIA + 1) <sup>***</sup> + log(Bathy) <sup>***</sup> + MSLA) <sup>ns</sup> + Slope <sup>***</sup> + SST <sup>***</sup>	1660	1.699 <sup>***</sup>	0.359	19.64	0.43 <sup>***</sup>
	Euphausiids	Biomass ~ log(ChIA + 1) <sup>***</sup> + log(Bathy) <sup>***</sup> + MSLA <sup>***</sup> + Slope <sup>***</sup>	614	1.392 <sup>***</sup>	0.172	37.48	0.61 <sup>***</sup>
	<i>M. norvegica</i>	Biomass ~ log(ChIA + 1) <sup>***</sup> + log(Bathy) <sup>***</sup> + MSLA) <sup>ns</sup> + Slope <sup>***</sup>	614	1.249 <sup>***</sup>	0.140	34.23	0.53 <sup>***</sup>
	<i>Thysanoessa</i>	Biomass ~ log(ChIA + 1))ns + log(Bathy) <sup>***</sup> + MSLA <sup>**</sup> + Slope <sup>***</sup> + SST <sup>*</sup>	614	0.957 <sup>***</sup>	0.231	27.11	0.44 <sup>***</sup>
<b>Summer</b>	Plankton	Biomass ~ log(ChIA + 1) <sup>***</sup> + log(Bathy) <sup>***</sup> + MSLA <sup>***</sup> + Slope <sup>***</sup> + SST <sup>*</sup>	2160	1.675 <sup>***</sup>	0.315	16.96	0.39 <sup>***</sup>
	Euphausiids	Biomass ~ log(ChIA + 1) <sup>***</sup> + log(Bathy) <sup>***</sup> + MSLA <sup>***</sup> + Slope <sup>***</sup> + SST <sup>***</sup>	2113	1.430 <sup>***</sup>	0.264	24.54	0.47 <sup>***</sup>
	<i>M. norvegica</i>	Biomass ~ log(ChIA + 1) <sup>***</sup> + log(Bathy) <sup>***</sup> + MSLA <sup>***</sup> + Slope <sup>***</sup> + SST <sup>***</sup>	2113	1.307 <sup>***</sup>	0.193	20.46	0.43 <sup>***</sup>
	<i>Thysanoessa</i>	Biomass ~ log(ChIA + 1) <sup>***</sup> + log(Bathy) <sup>***</sup> + MSLA <sup>***</sup> + Slope <sup>***</sup> + SST <sup>***</sup>	2113	0.876 <sup>***</sup>	0.325	26.47	0.49 <sup>***</sup>

*p*-value of smooth terms and correlation coefficients are indicated by : ns > 0.05; \* 0.05 - 0.01; \*\* 0.01 - 0.001; \*\*\* < 0.001  
r: Spearman rank correlation coefficient.

Tables 2: Optimal GAMs based on krill biomass data. Environmental data range showing partial residuals > 0 indicating a positive effect on biomass of the different krill categories in spring (May-June) and summer (July-August-September). The absence of values = variable not selected in a particular GAM. See text for the description of abbreviations used for environmental variables.

Category	Variables	Spring min	max	Summer min	max
Euphausiids	ChlA	2.78	-	4.05	23.05
	Bathy	62	228	69	233
	MSLA	0.049	0.064	-0.047	0.073
	Slope	0.35	1.31	0.32	1.85
	SST	-	-	10.9	16.2
<i>M. norvegica</i>	ChlA	2.97	-	4.37	21.65
	Bathy	69	324	74	473
	MSLA	-	-	-0.053	0.074
	Slope	0.36	2.67	0.35	1.955
	SST	-	-	9.8	16
<i>Thysanoessa</i>	ChlA	-	-	4.21	32.78
	Bathy	56	172	60	200
	MSLA	0.053	0.07	-0.055	0.06
	Slope	0.3	0.83	0.3	1.75
	SST	10.5	-	11.2	16.2

FIGURES

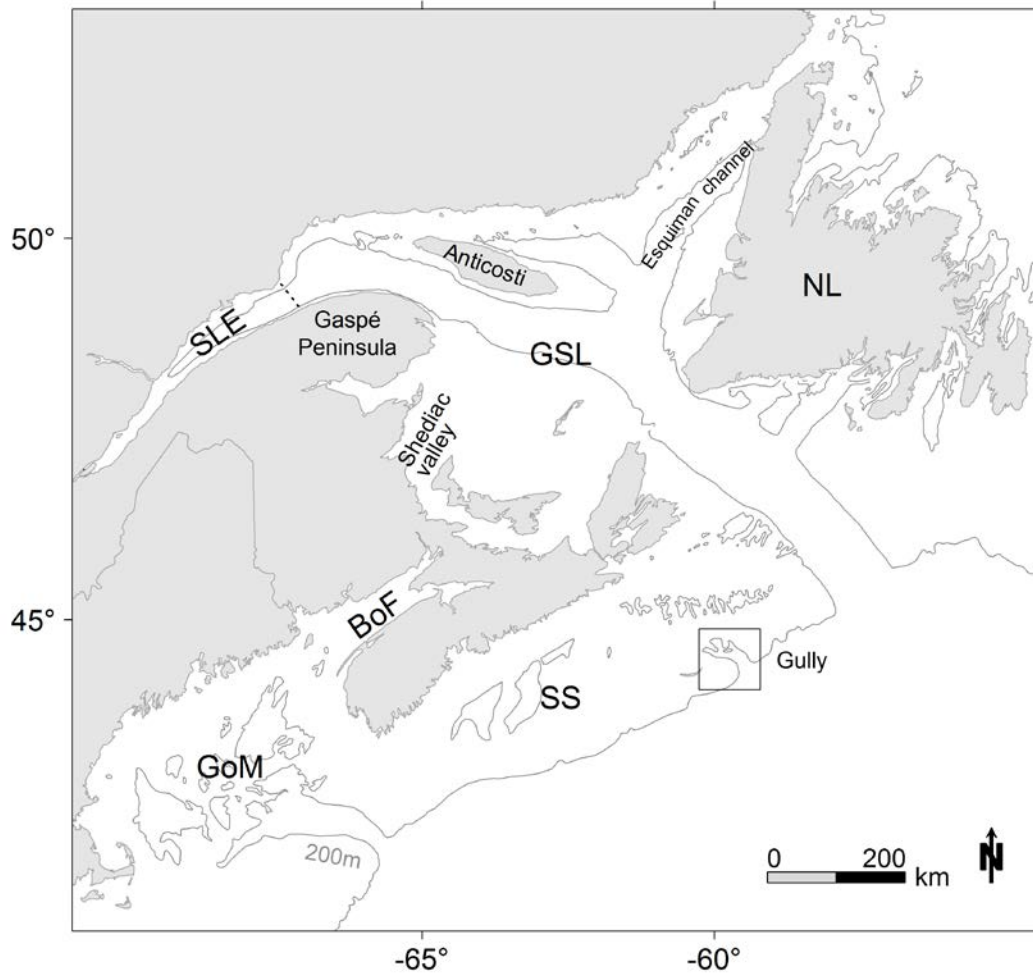


Figure 1: Map of the study area and regions. BoF: Bay of Fundy, GoM: Gulf of Maine, GSL: Gulf of St. Lawrence, NL: Newfoundland, SLE: Lower St Lawrence Estuary, SS: Scotian Shelf. Grey lines represent the 200 m isobath.

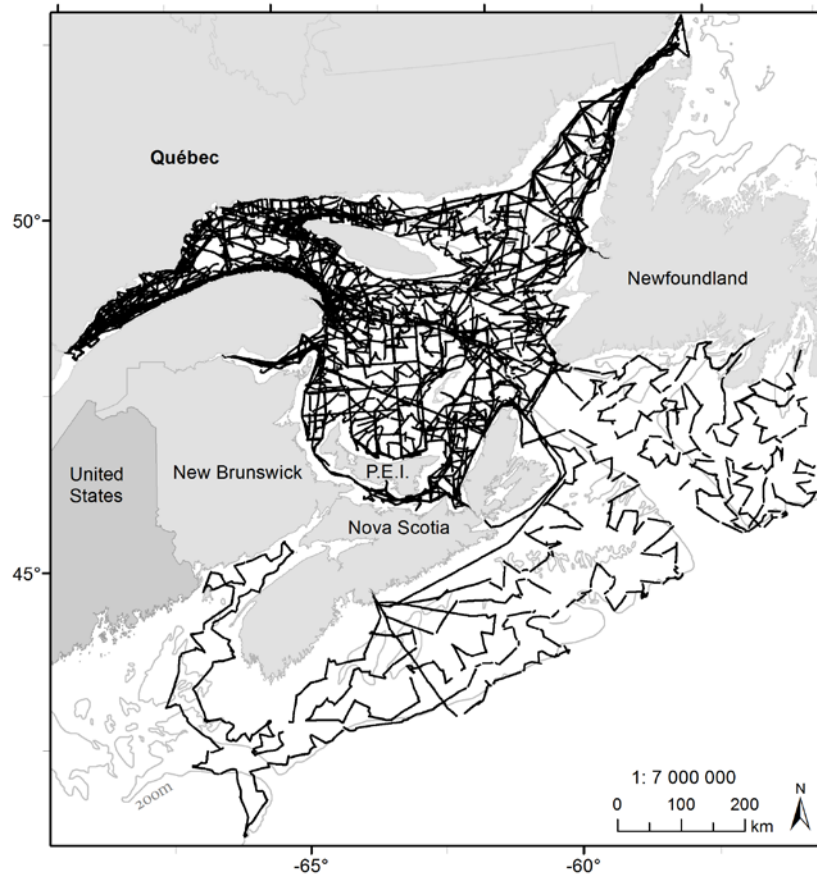


Figure 2: Vessel tracks for various acoustic surveys conducted in eastern Canada (Plourde et al. unpublished data).

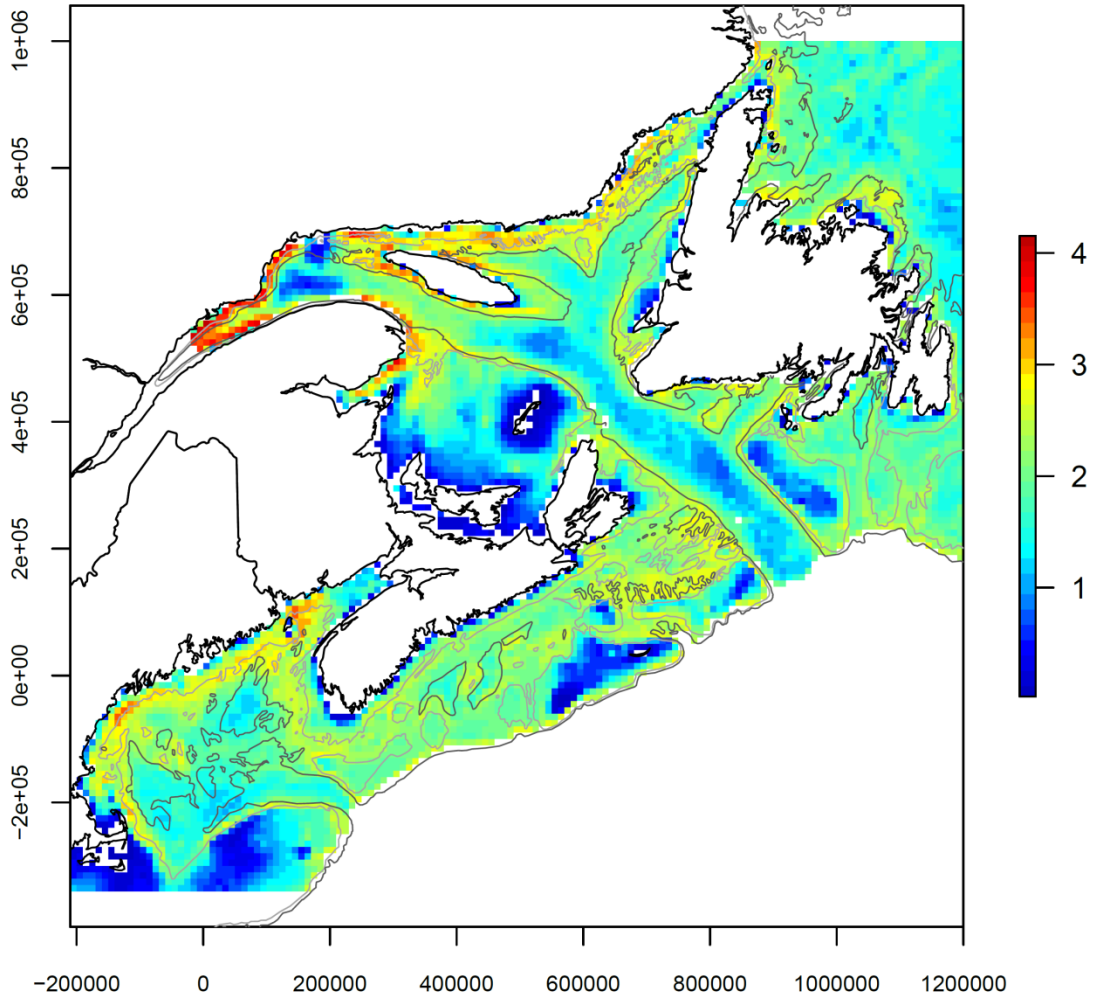


Figure 3: Biomass ( $\text{g m}^{-2}$ ) for the krill category Euphausiids' predicted in June 2012 with the GAM built with acoustic data collected in May and June in the GSL. Biomass represented as  $\text{Ln}(x+1)$ .

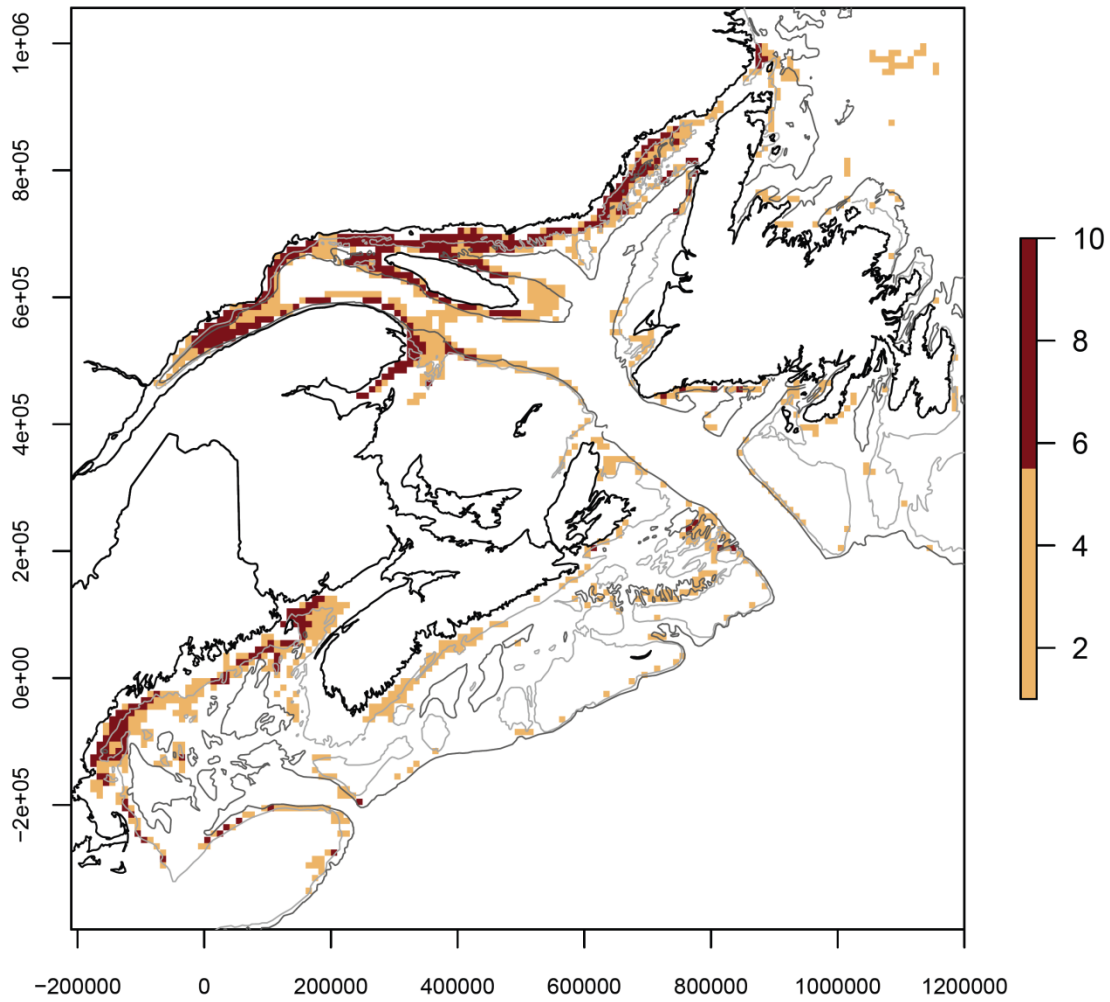


Figure 4: Euphausiids in spring. Locations with a probability greater than 50% for a dense krill aggregation (biomass >95<sup>th</sup> percentile) to occur (red) and defined as Significant Areas of Krill (SAK) in spring 2009-2013. Predictions were performed with the GAM described in Table 2. Dark grey line: 200 m isobaths. Light grey line: 100 m isobaths.



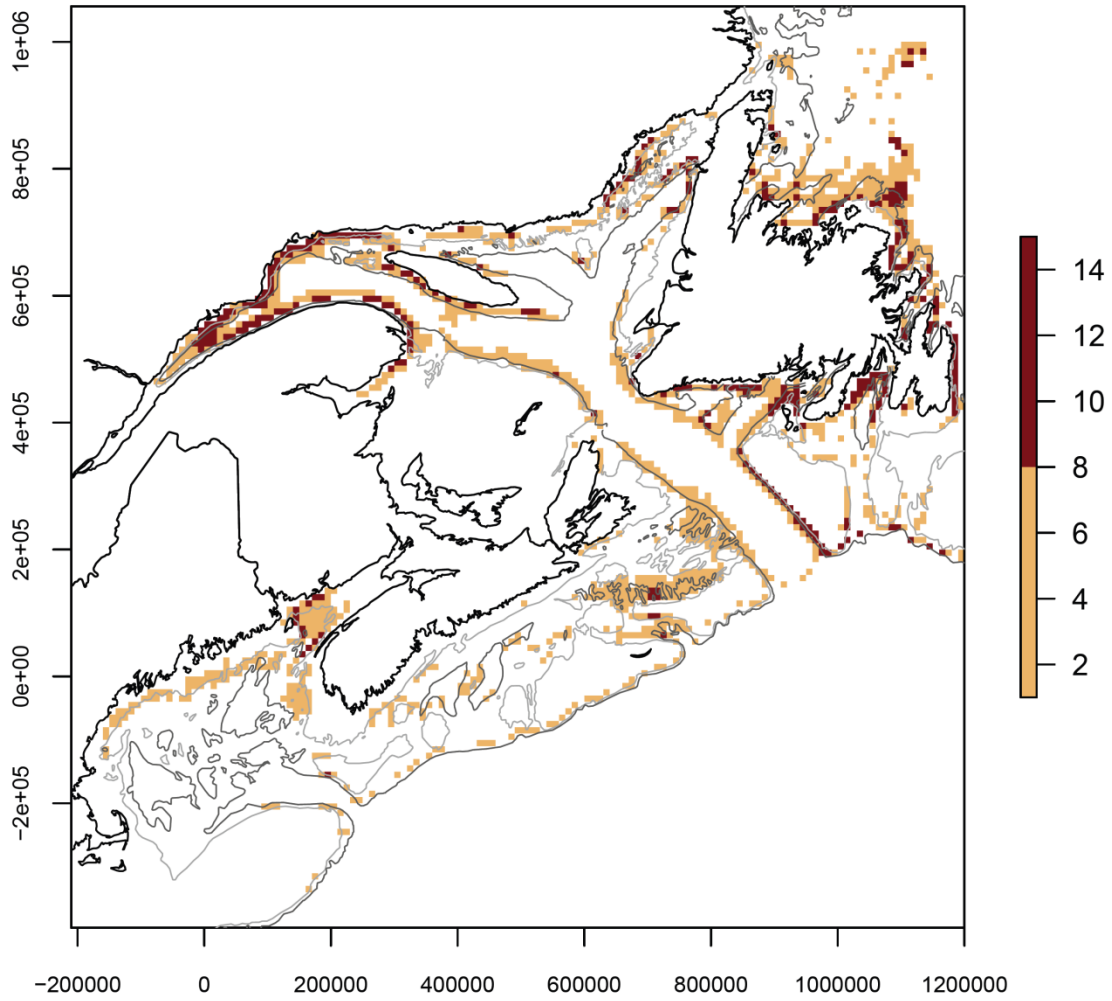


Figure 5: Euphausiids in summer. Locations of SAK in summer 2009-2013. Predictions were performed with the GAM described in Table 2. See Fig. 3 caption for layout details.

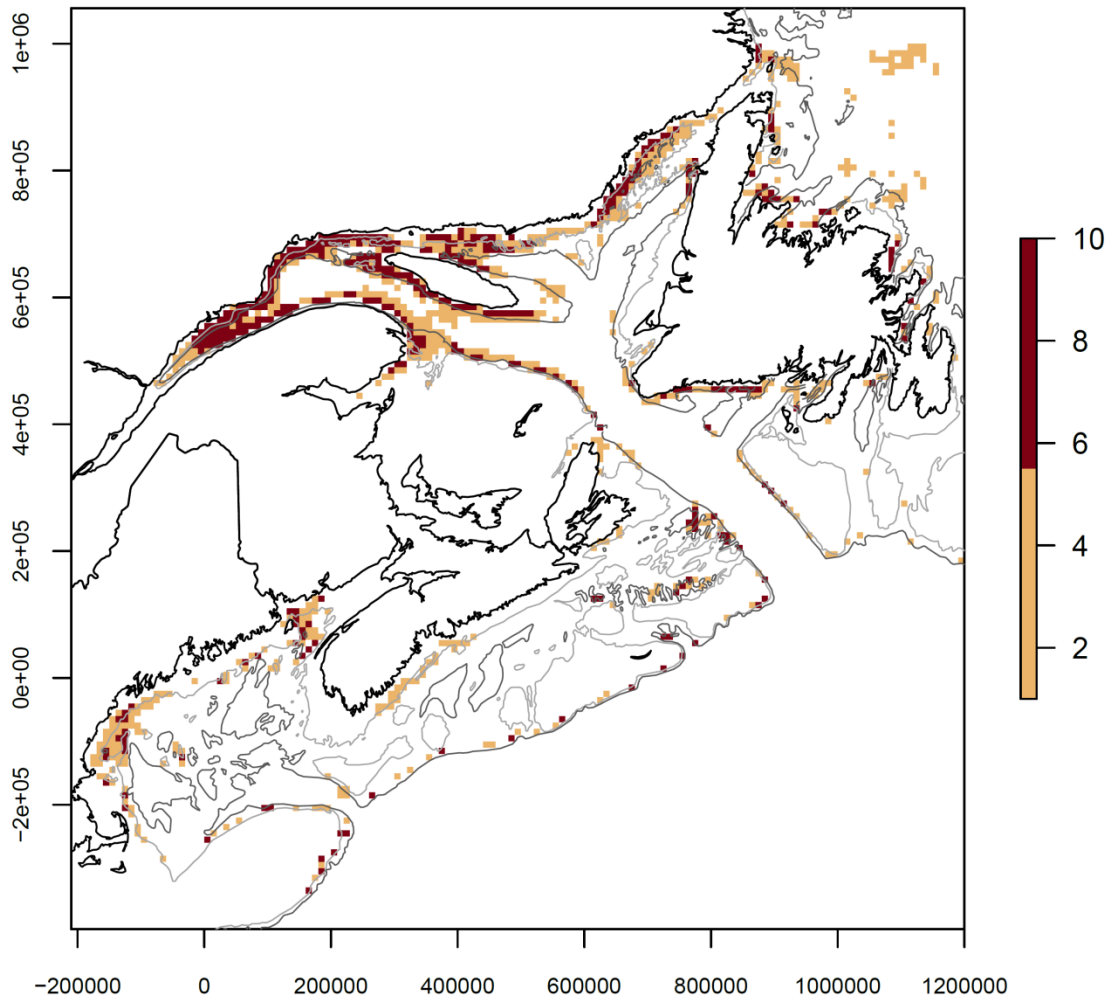


Figure 6: *Meganyctiphanes norvegica* in spring. Locations of SAK in spring 2009-2013. Predictions were performed with the GAM described in Table 2. See Fig. 3 caption for layout details.

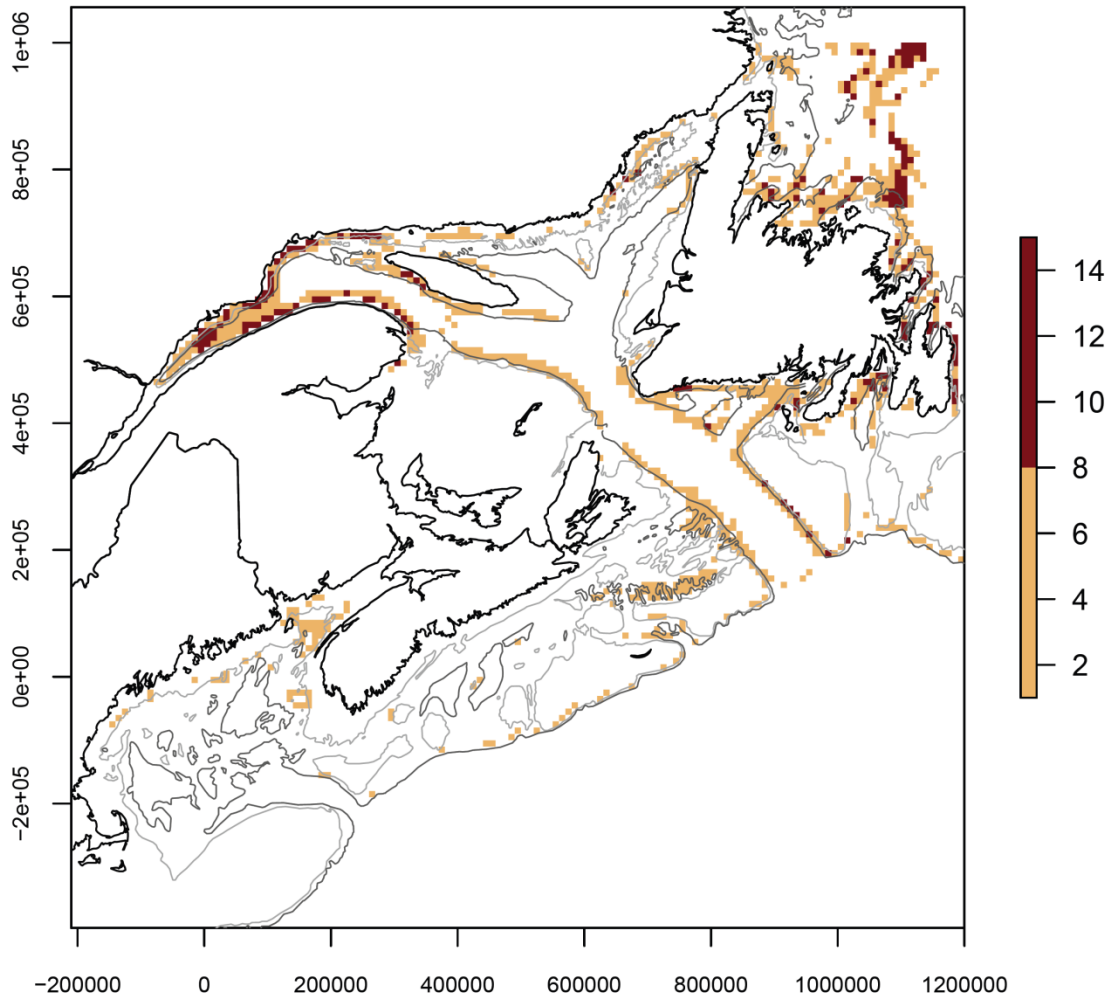


Figure 7: *Meganyctiphanes norvegica* in summer. Locations of SAK in summer 2009-2013. Predictions were performed with the GAM described in Table 2. See Fig. 3 caption for layout details.

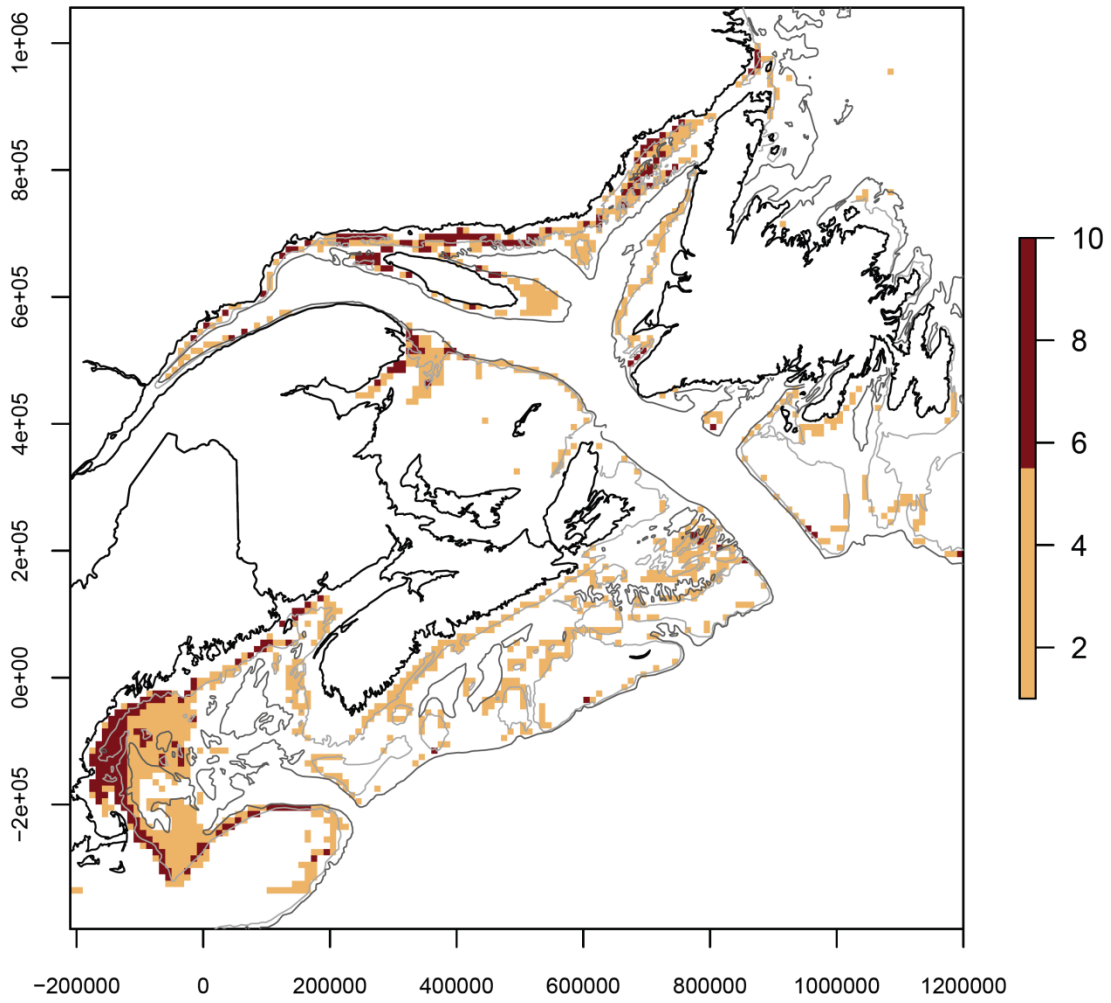


Figure 8: *Thysanoessa* spp. in spring. Locations of SAK in spring 2009-2013. Predictions were performed with the GAM described in Table 2. See Fig. 3 caption for layout details.

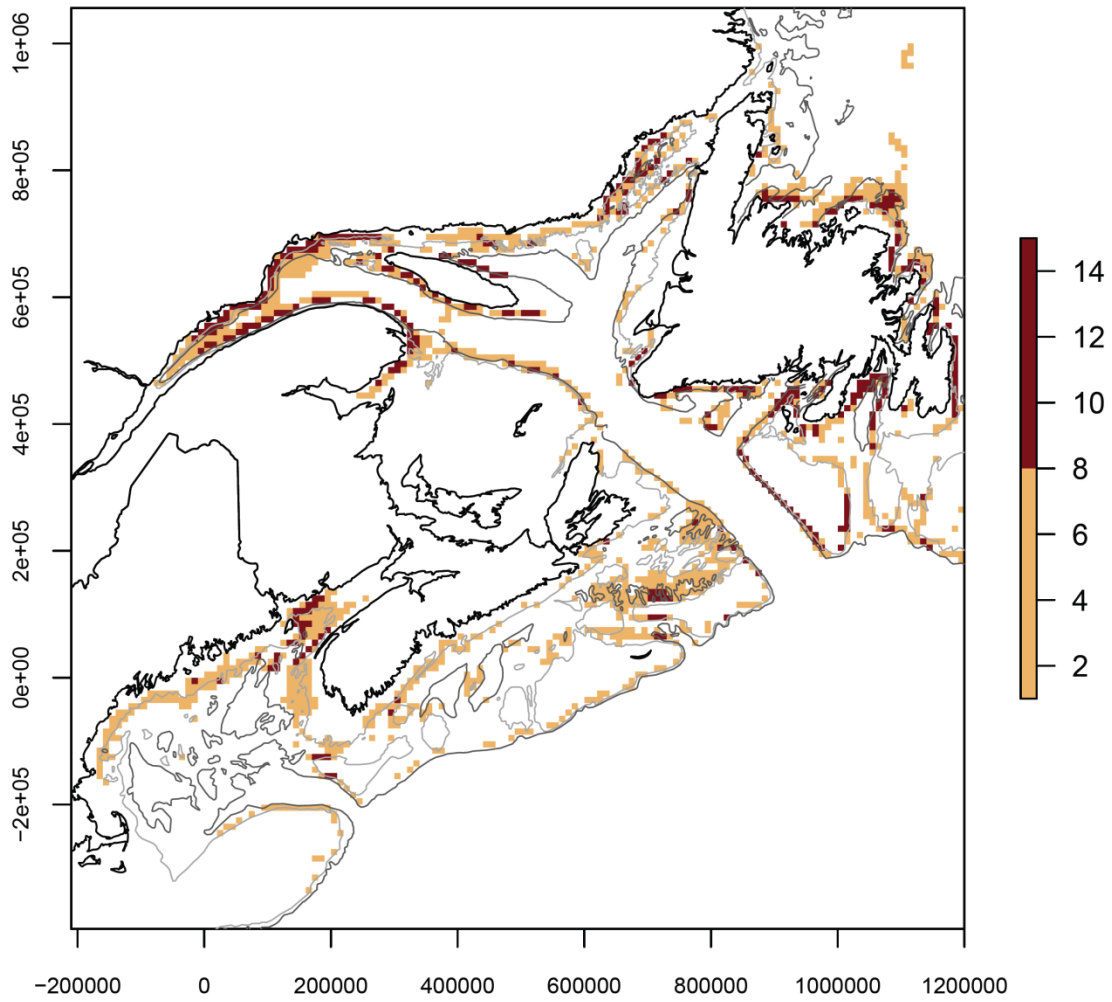
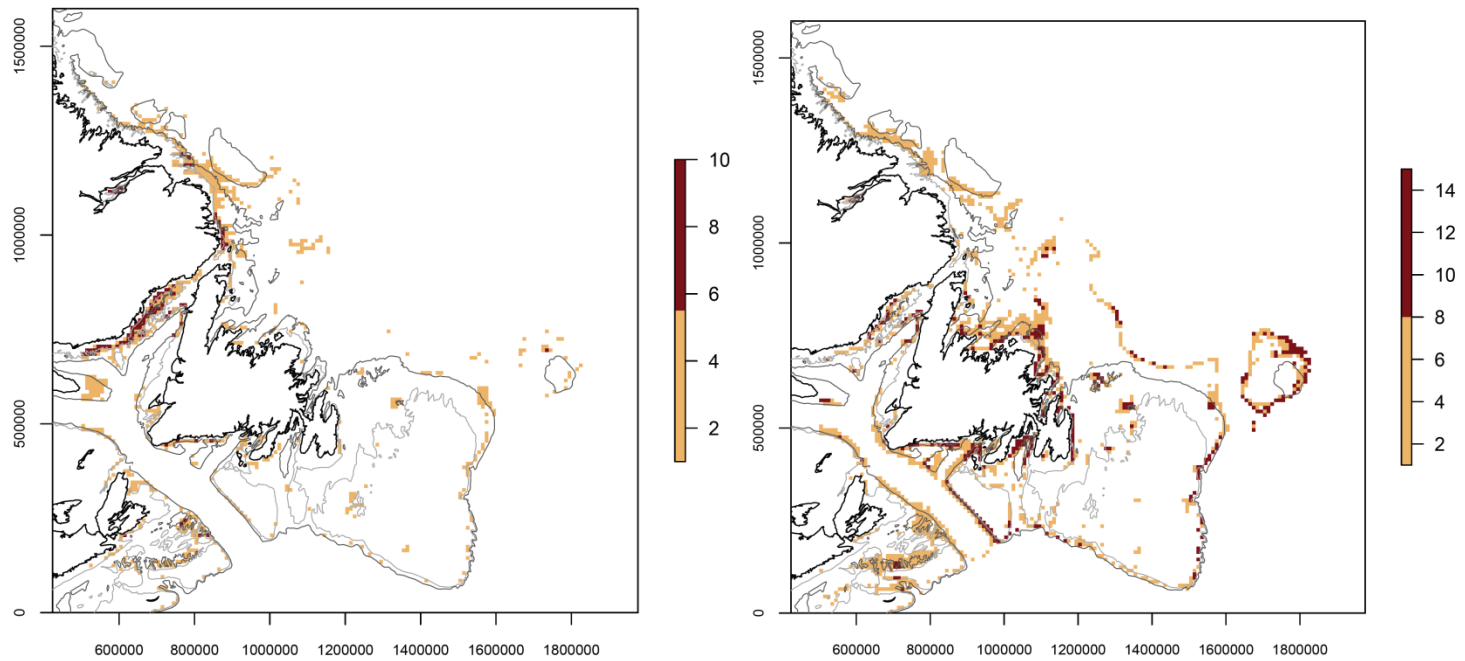
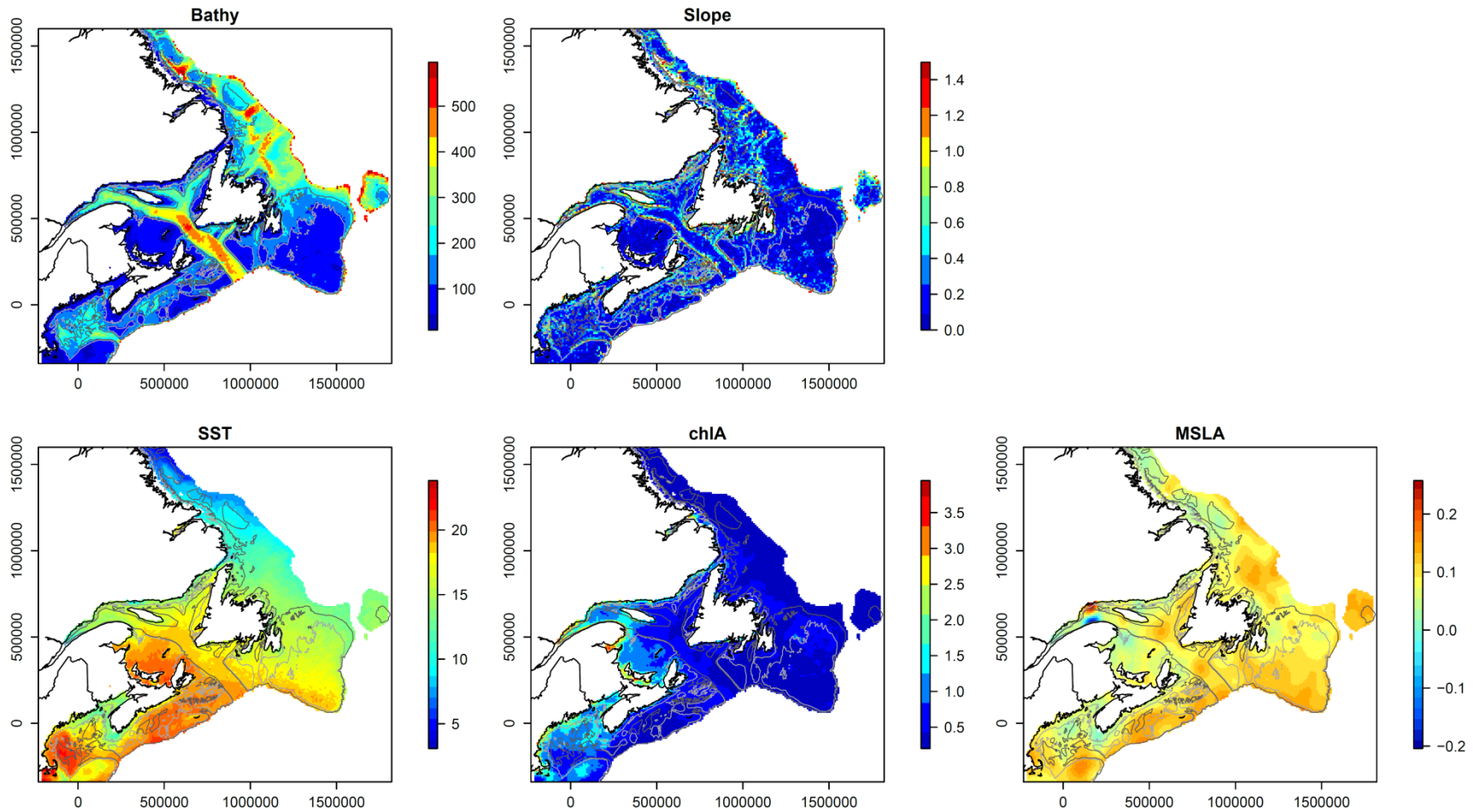


Figure 9: *Thysanoessa* spp. in summer. Locations of SAK in summer 2009-2013. Predictions were performed with the GAM described in Table 2. See Fig. 3 caption for layout details.

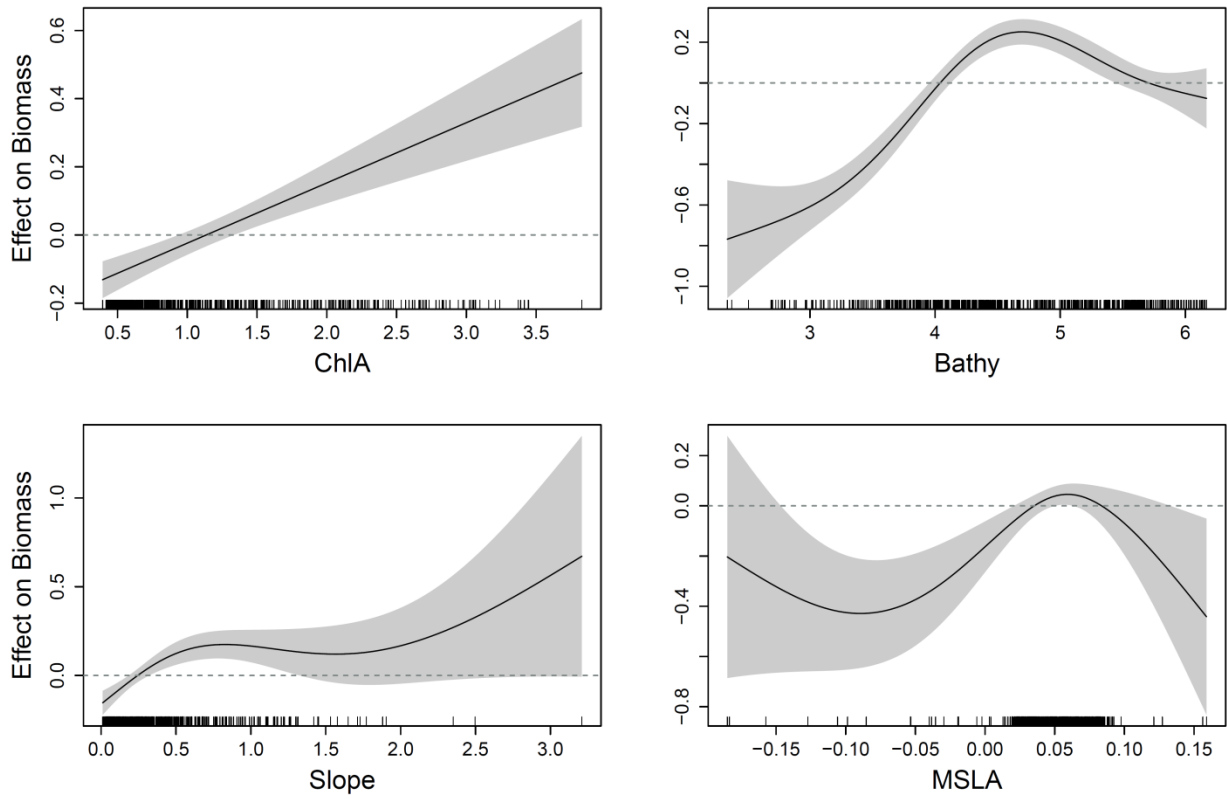


*Figure 10: Euphausiids on the eastern Newfoundland shelf. Locations of SAK in spring (left panel) and summer (right panel) 2009-2013. Predictions were performed with the GAM described in Table 2. See Fig. 3 caption for layout details.*

## APPENDIX

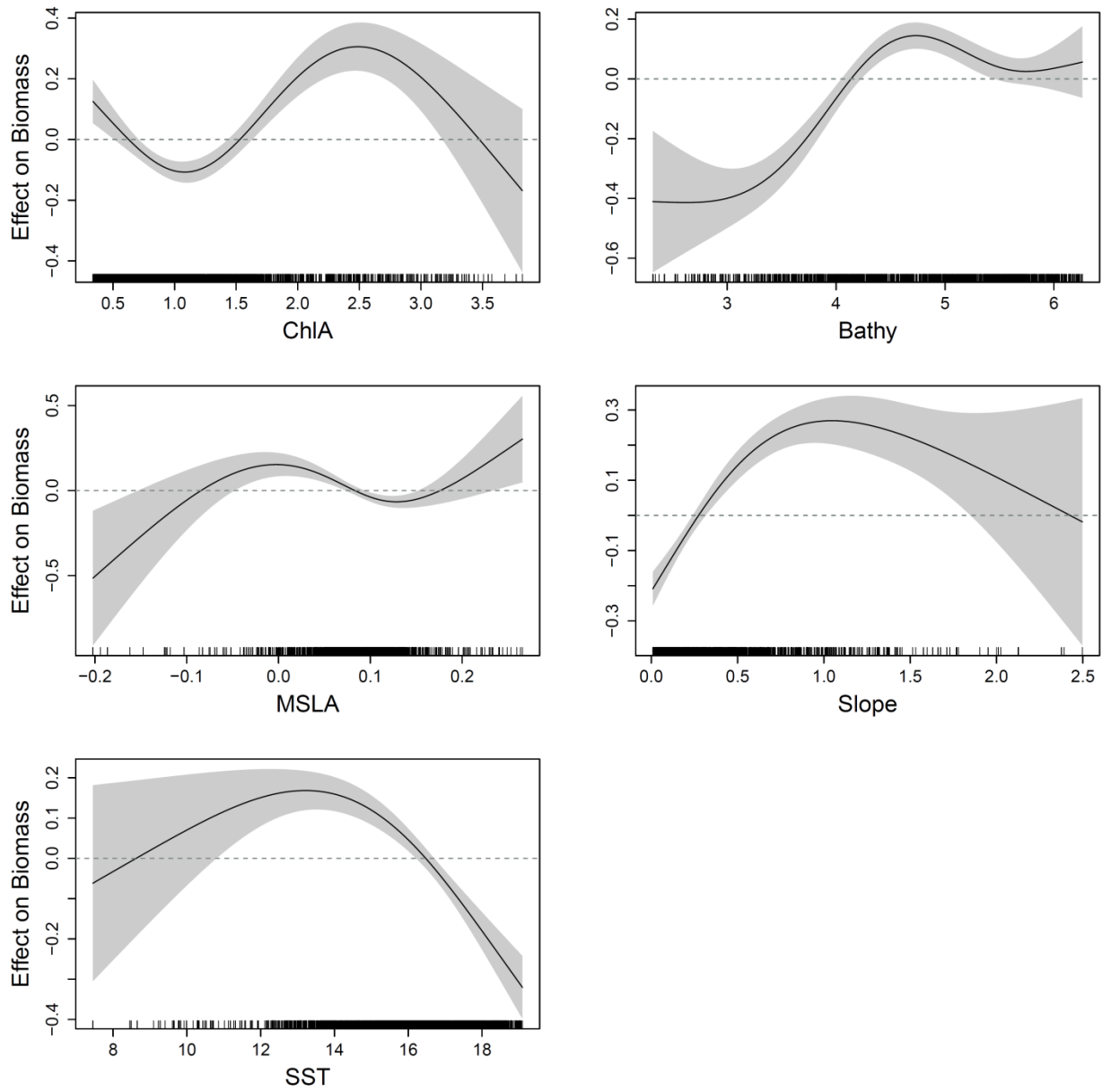


Appendix 1: Spatial patterns of static (Bathy, Slope: upper panels) and dynamic (SST, CHLA, MSLA: lower panels) environmental variables used in krill habitat models. Dynamic variables are averaged for August 2012 as an example of their spatial structure. Data are represented on a 10\*10km cell grid.

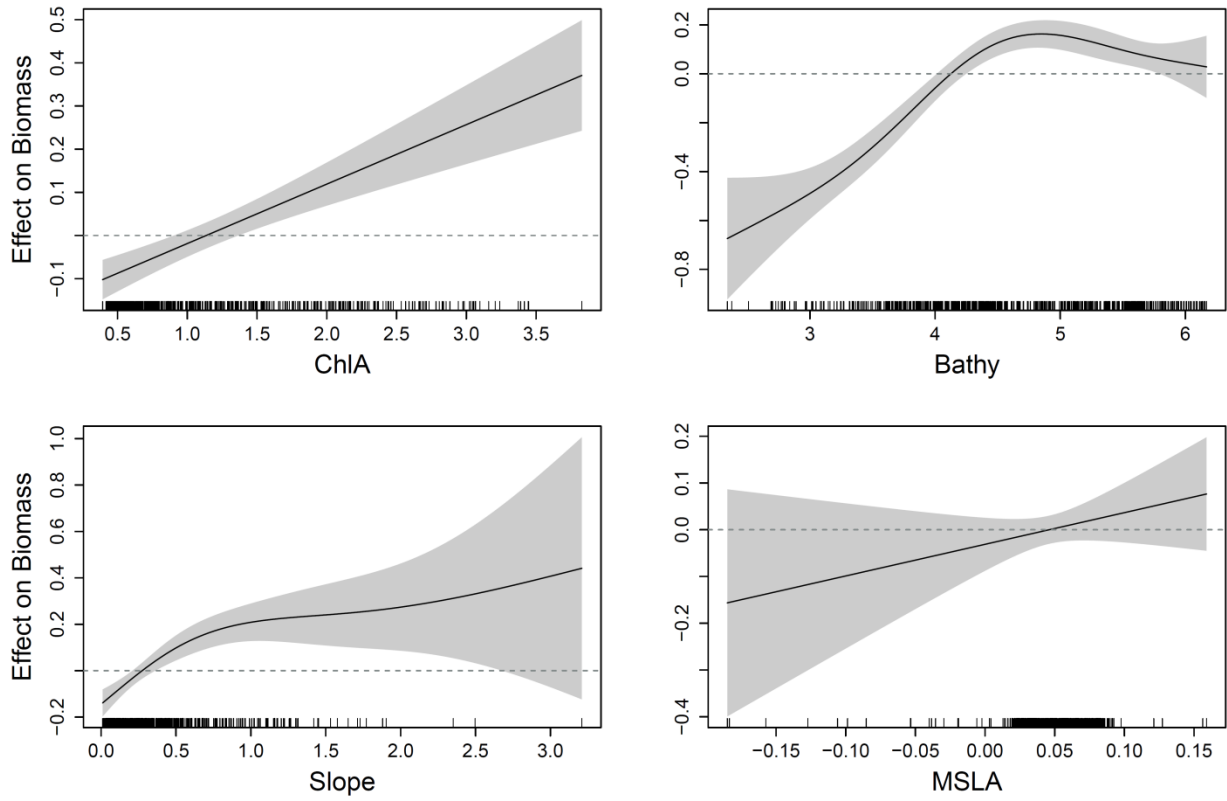


*Appendix 2: Optimal GAM showing the influence of significant environmental on biomass of krill in the Euphausiids category during the spring period. Ticks on the x-axis indicated the data observations. The environmental variable has no effect when the 95% confidence intervals (shaded areas) include the zero on the y-axis (dotted line). See Table 1 for GAMs details.*

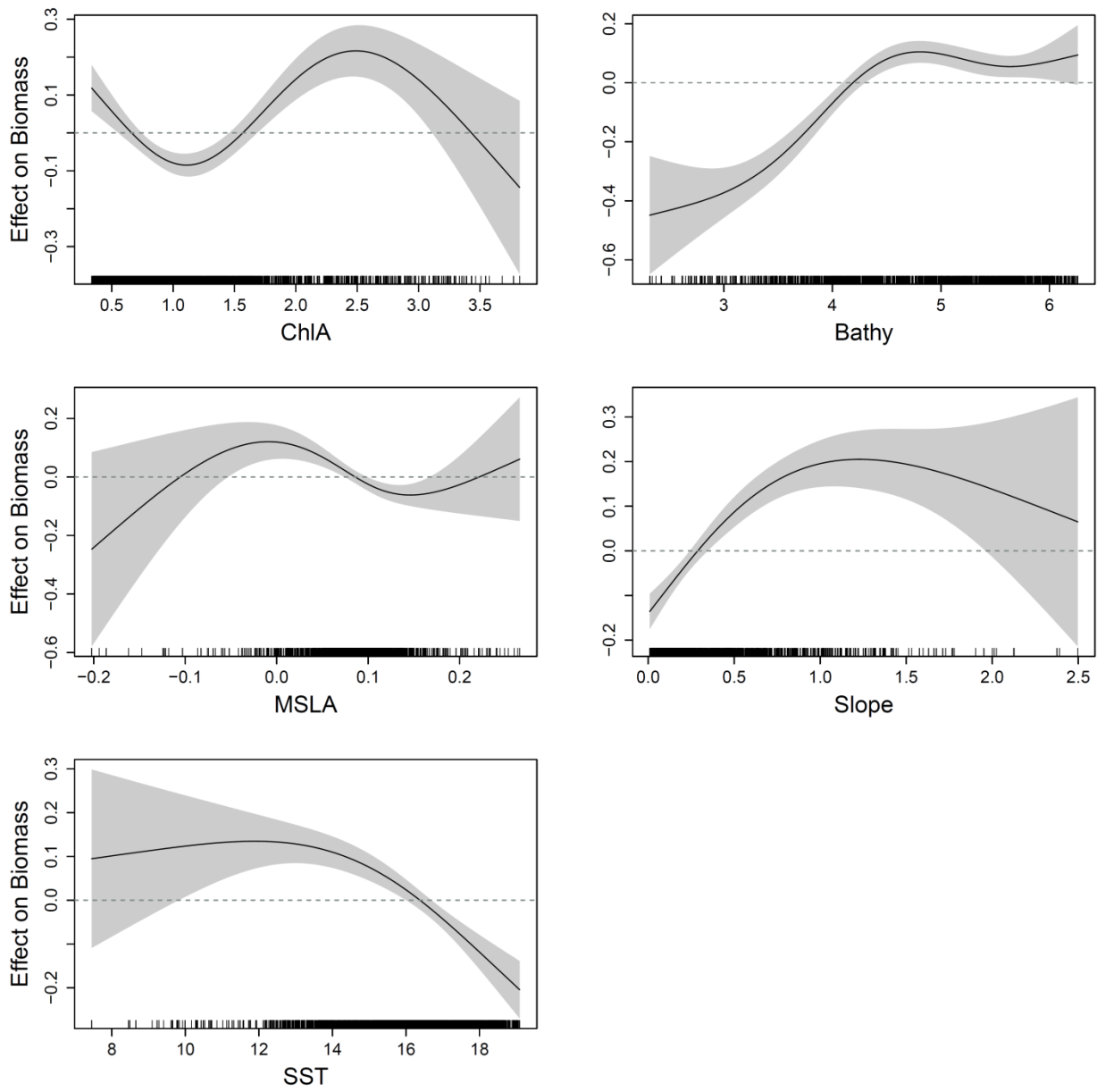




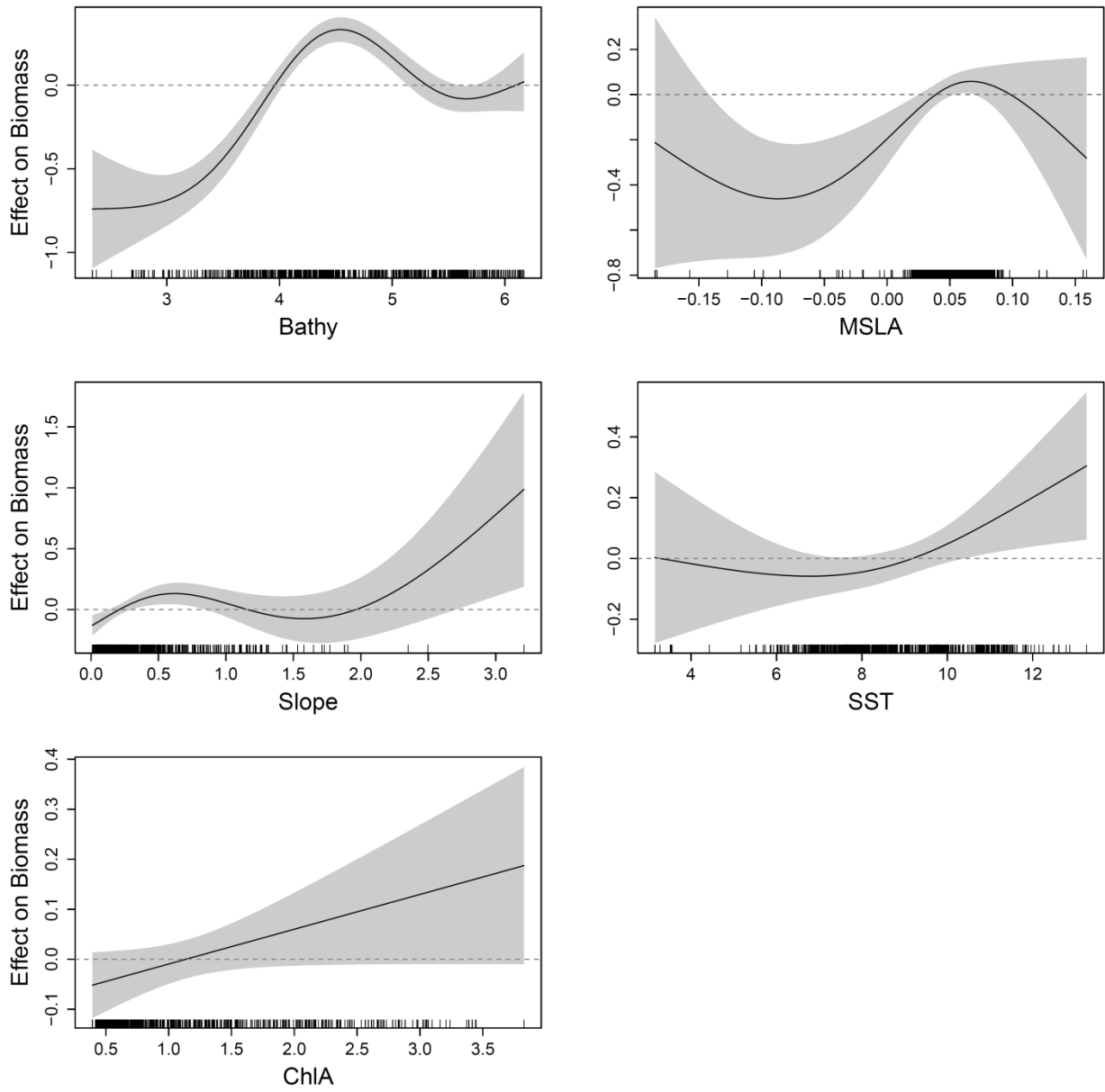
Appendix 3: Optimal GAM showing the influence of significant environmental on euphausiids biomass during the summer period. See Appendix 2 caption for details of figure layout.



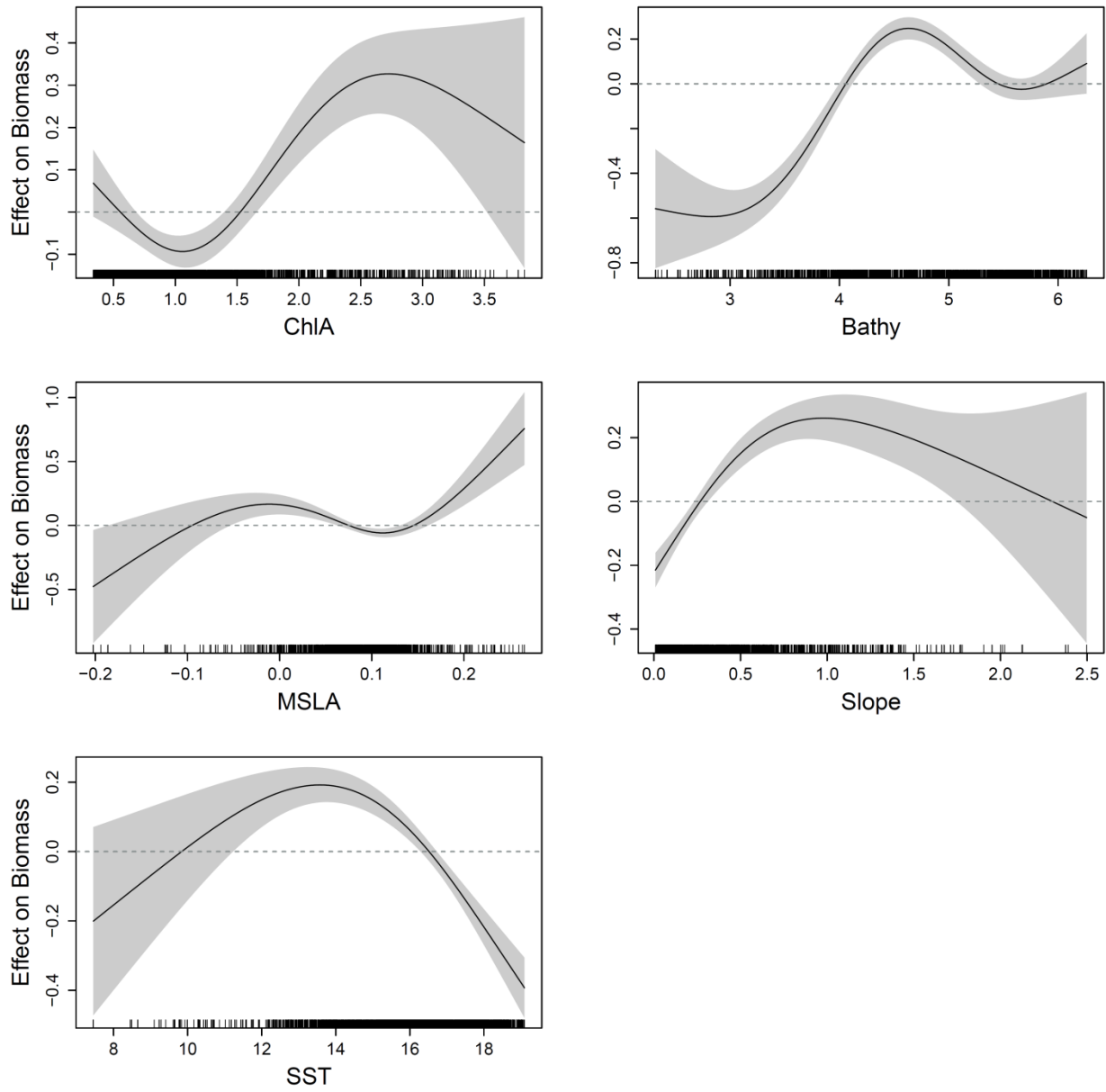
Appendix 4: Optimal GAM showing the influence of significant environmental on *Meganyctiphanes norvegica* biomass during the spring period. See Appendix 2 caption for details of figure layout.



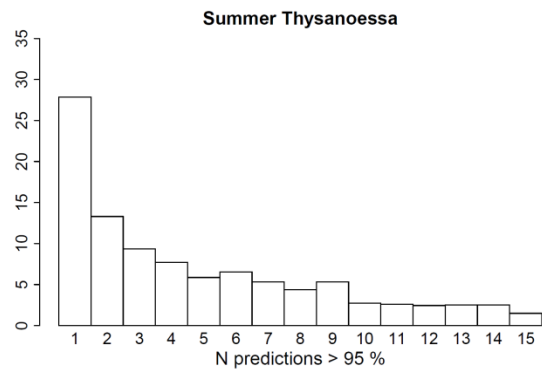
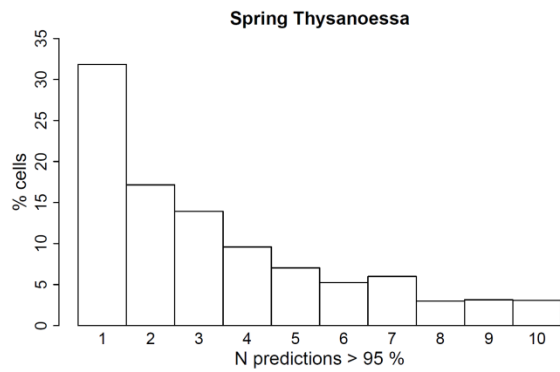
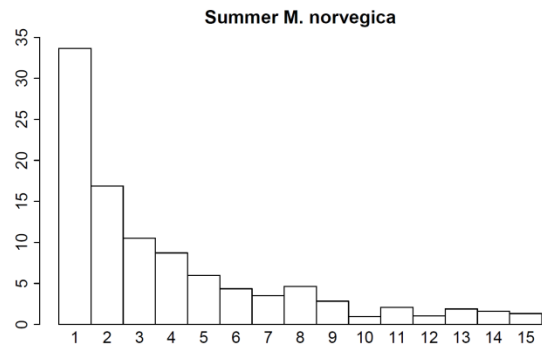
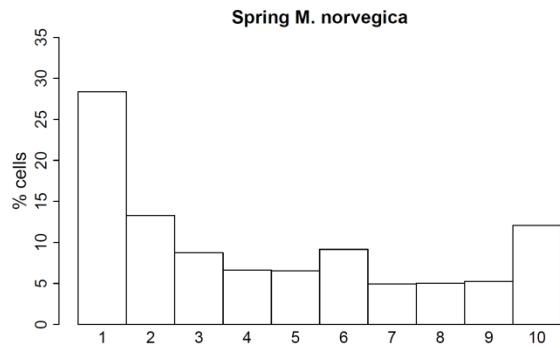
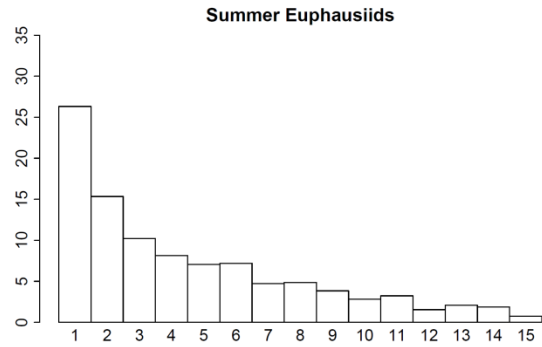
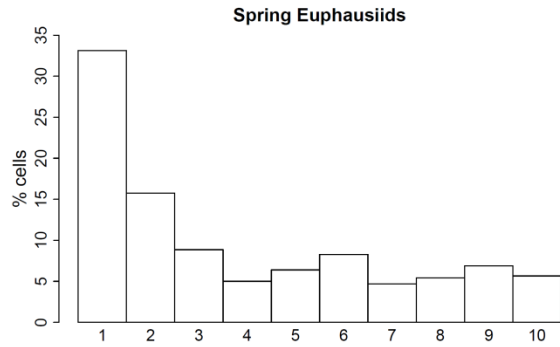
Appendix 5: Optimal GAM showing the influence of significant environmental on *Meganyctiphanes norvegica* biomass during summer. See Appendix 2 caption for details of figure layout.



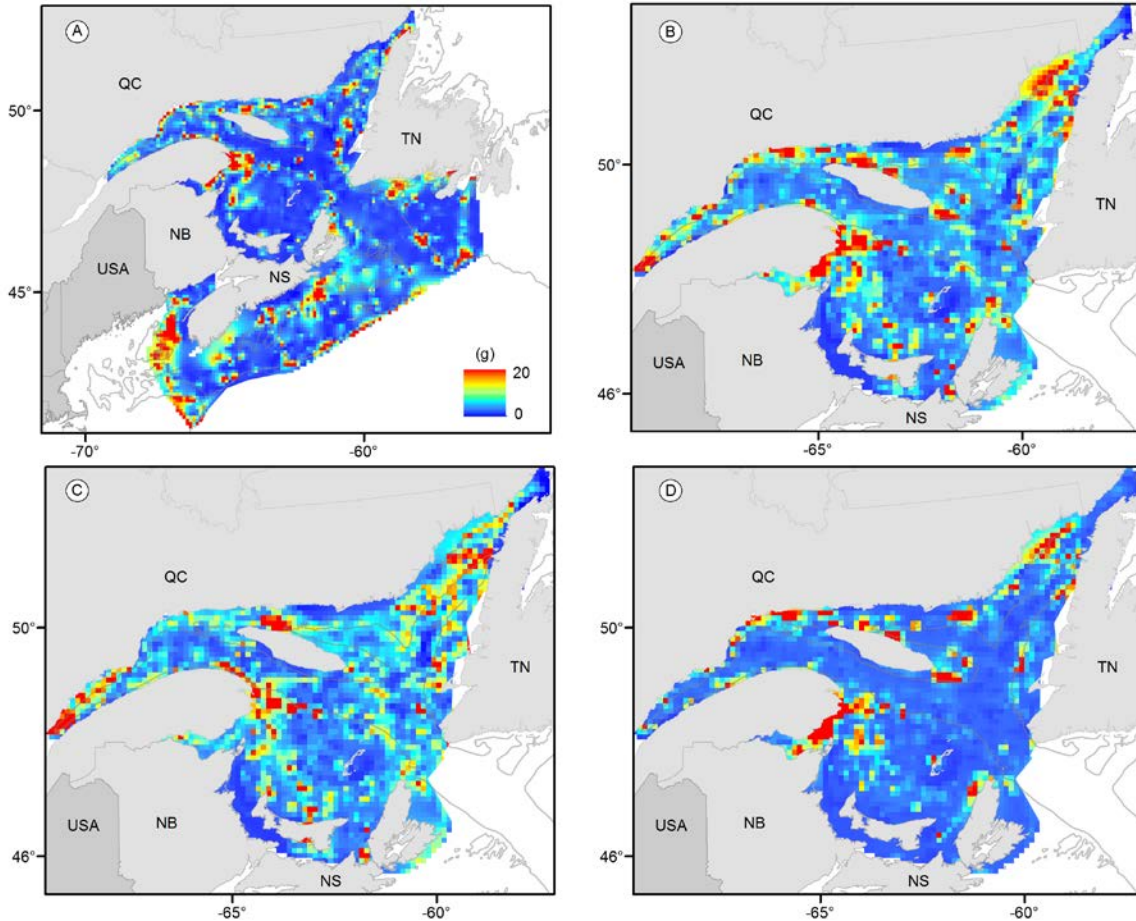
Appendix 6: Optimal GAM showing the influence of significant environmental on *Thysanoessa* species biomass during spring. See Appendix 2 caption for details of figure layout.



Appendix 7: Optimal GAM showing the influence of significant environmental on *Thysanoessa* species biomass during summer. See Appendix 2 caption for details of figure layout.



Appendix 8: Frequency distribution of the number of krill biomass >95<sup>th</sup> percentile predicted in each grid cells with GAMs built for krill categories of Euphausiids, *M. norvegica* and *Thysanoessa* species in spring and summer. Significant Areas of Krill (SAK) = cells with > 5 and > 8 high biomass values in spring and summer respectively. Frequency of grid cells with no krill biomass >95<sup>th</sup> percentile represented 90% of the domain and were not plotted.



Appendix 9: Spatial distribution of krill biomass based on acoustic data for the Plankton category estimated with dual frequency acoustic in the GSL, SS-Bay of Fundy and Newfoundland (A), and for the Euphausiids (B), *M. norvegica* (C) and *Thysanoessa* spp (D) categories estimated with multifrequency acoustic in the GSL. Data are represented as standardized anomalies ( $\pm$  number of s.d) of the maximum krill biomass ( $\text{g m}^{-2}$ ) observed in each  $10^{\circ} \times 10^{\circ}$  km cell relative to the average value over the entire spatial domain (Plourde et al.<sup>1</sup> unpublished report).

<sup>1</sup> Plourde, S., McQuinn, I.H., Lesage, V., Lehoux, C., Joly, P., Bourassa, M-N. Spatial distribution of krill in eastern Canadian waters: a climatological approach based on historical plankton net and acoustic data. Institut Maurice Lamontagne, 850 route de la mer, Mont-Joli, Qc, G5H 3Z4